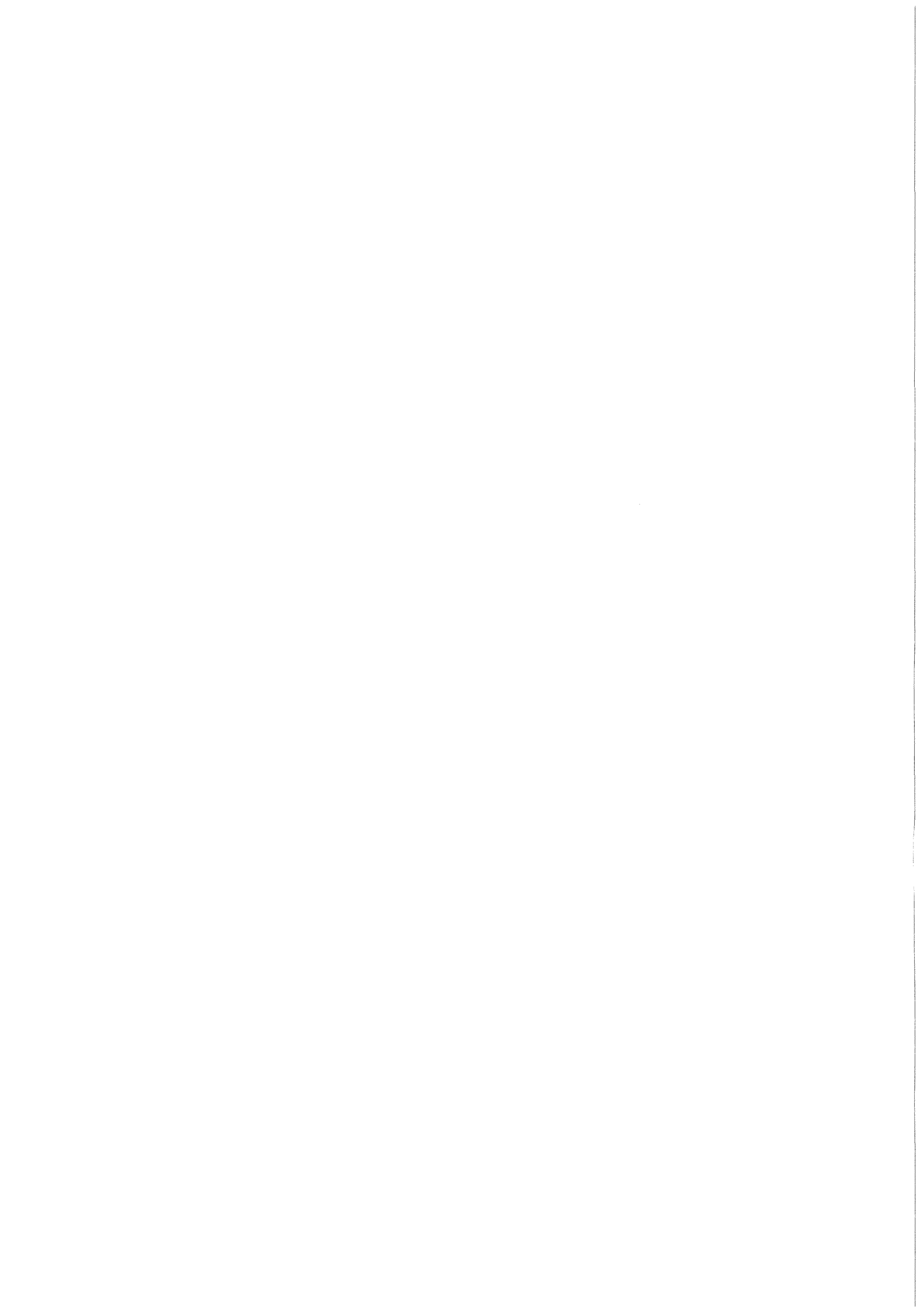


KfK 3620
Mai 1984

Analysis of the Multiplication of D-T Neutron Sources in Blanket Materials of Fusion Reactors

M. Segev
Institut für Neutronenphysik und Reaktortechnik

Kernforschungszentrum Karlsruhe



KERNFORSCHUNGSZENTRUM KARLSRUHE
Institut für Neutronenphysik und Reaktortechnik

KfK 3620

ANALYSIS OF THE MULTIPLICATION OF D-T NEUTRON SOURCES
IN BLANKET MATERIALS OF FUSION REACTORS

M. Segev*

* delegated from Ben-Gurion University of the Negev
Beer-Sheva, Israel

Kernforschungszentrum Karlsruhe GmbH., Karlsruhe

Als Manuskript vervielfältigt
Für diesen Bericht behalten wir uns alle Rechte vor

Kernforschungszentrum Karlsruhe GmbH
ISSN 0303-4003

ABSTRACT

A D-T neutron source is amplified when emitted into a body of material with appreciable (n,2n), (n,3n) or (n,f) cross sections. This amplification is described by a simple theory, approximating the strict integral transport description of the process. The distribution of neutrons in energy, from 14 MeV down to the (n,2n) threshold, is approximated by effective one-group cross sections for amplifiers of high and medium mass numbers; two-group cross sections are needed for Be. The spatial character of the multiplication is described by average collision probabilities for non-flat collision sources. The probabilities are approximated for spherical shell geometry with a small number of geometrical parameters.

The theory enables a very accurate determination of $\sigma_{n,2n} + 2\sigma_{n,3n} + (v_f - 1)\sigma_f$ at the source energy from measurements of total multiplications. If total leakages above the (n,2n) threshold are also measured, then the hardness of the secondary neutron spectra can be estimated.

The accuracy of the approximate theory was ascertained by energy-space detailed transport comparison calculations for Be, Cu, Zr, Fe, Pb and U238.

Untersuchungen zur Multiplikation von Neutronen einer D-T-Neutronenquelle in Blanketmaterialien von Fusionsreaktoren

ZUSAMMENFASSUNG

In Materialien mit merklichen $(n,2n)$, $(n,3n)$ oder (n,f) Reaktionswirkungsquerschnitten wird die Anzahl von Neutronen vergrößert werden. Diese Neutronenmultiplikation wird hier durch eine einfache Theorie beschrieben, die die strenge Beschreibung durch die integrale Transporttheorie annähert. Für Materialien mit hoher und mittlerer Massenzahl werden die energieabhängigen Reaktionsquerschnitte durch einen effektiven Eingruppenquerschnitt beschrieben, für Be ist eine Darstellung mit zwei Energiegruppen notwendig. Die räumliche Abhängigkeit des Multiplikationseffektes wird durch mittlere Stoßwahrscheinlichkeiten berechnet, wobei die Stoßquellen nicht als räumlich konstant angenommen werden. Die Stoßwahrscheinlichkeiten werden für sphärische Geometrie durch eine kleine Zahl von Geometrieparametern angenähert.

Aus den Messungen der Gesamtmultiplikation kann man mit Hilfe dieser Theorie für die Quellenergie sehr genau den Wert von $\sigma_{n,2n} + 2\sigma_{n,3n} + (v_f - 1)\sigma_f$ bestimmen. Wenn die Gesamtneutronenleckage oberhalb der $(n,2n)$ -Schwelle ebenfalls gemessen wird, kann man die Härte des Sekundärneutronenspektrums abschätzen.

Die Zuverlässigkeit des Näherungsverfahrens wurde für die Neutronenmultiplikation an Be, Cu, Zr, Fe, Pb und U 238 mit Hilfe genauerer Transportrechnungen nachgewiesen.

Contents

Abstract	
Introduction	1
Chapter I : Theory	3
Chapter II : Collision Probabilities	13
Chapter III: Analysis of the Neutron-Amplification in Pb,Zr,Cu,Fe, U238 and Be	20
Chapter IV : The Role of the Theory in the Analysis of Multiplication Experiments	24
Chapter V : Analysis of Takahashi's Neutron Multiplication Experiments in Pb	28
Chapter VI : Conclusions	34
References	37
Appendix	38
Tables	40
Graphs	59

Introduction

Conceptual designs of D-T fusion devices often call for enhancement of the D-T neutron output, prior to entering the Tritium breeding zone. With late indications of poorer (n,t) cross sections in lithium ^{/1/} the pre-amplification of the 14 MeV neutron source becomes almost inevitable. There are a few competitor elements for the role of amplifiers, each presenting prospects and problems. Current neutron data for Be makes it a prime candidate, but it has material problems. Pb has gained attention recently, due to measurements ^{/2/} which show a better amplification than judged by its current neutron data. The actinides, U238 and Th232 for example, though highly amplifying, present radiation and proliferation problems. Other, poorer, amplifiers should also be studied as they may be used as alloy, or structural constituents in the pre-amplification zone.

Neutron amplification comprises many aspects ^{/3-6/}. For example, in two of these, the benchmarking of differential data vs. experimental integral data and the optimal design of a fusion blanket, the calculational tool requires a rigorous space-energy transport code. Other aspects, such as the experimental determination of partial neutron data, the comparison between the amplification properties of different materials, and general design considerations, could be based on a simpler approximate calculational tool.

The theory presented in this article is a simple approximate calculational tool. Approximations are made in the description of the space-energy distribution of the neutrons, as they spread away from the assumed localized monoenergetic source by repeated collisions in the material body. Simplicity comes as a result of the approximations made, and of certain features of the energy dependence of the cross sections.

The basic theory is developed in section I. The amplification of the source depends critically on the average collision probability for the source neutrons. Second in importance is the average collision probability for the neutrons after their first collision. This probability is often close in magnitude to the fundamental-mode type, "stationary", average collision probability, approached within a few collisions ^{/7,8/}. Neutrons are assumed to scatter isotropically.

The slowing down process from the source to the (n,2n) threshold energy is approximated by an equation similar to the infinite-medium slowing down equation, with group-dependent average collision probabilities taking up the role of absorption fractions.

The average collision probabilities are discussed in section II. In diffusion theory the collision probability for a fundamental-mode source is a rational expression, namely $\Sigma/(\Sigma + \Sigma_g)$, with $\Sigma_g = B^2/3\Sigma$, where Σ is the macroscopic transport cross section and B^2 is the geometrical buckling of the body. Approximately then $1/\Sigma_g = \alpha l + \beta l^2$, where l is the mean optical chord length of the body and α and β are numerical coefficients. Kumar^{/9/} has fitted the parameters for cuboids, spheres, cylinders, and slabs of all thicknesses. In this paper α and β are fitted for spherical shells. Further, the average probability of first collisions in the spherical shell is shown to be also of the approximate form $\Sigma/(\Sigma + \Sigma_g)$, where now $1/\Sigma_g = \alpha l + \beta l^2 + \gamma l^3$, α and β being the same coefficients as for the fundamental mode source probability.

The results of sections I and II are used in section III to describe in simple terms the multiplication of D-T neutron sources in spherical shell of Be, Cu, Fe, Zr, Pb and U238. ENDF/B-IV data taken as basis, accurate multiplications were calculated with a P3/S16 transport approximation for a central source in the shells. The space-integrated energy distributions, evaluated by the method of section I, well compare with the transport code results. Favourable cross section features enable the use of one energy group to calculate the amplification in Cu, Fe, Zr, Pb, U238, and two groups for Be.

The possible role of the theory in the analysis of experiments is discussed in section IV. In order to determine the number of secondaries produced at the source energy, a measurement of the total multiplication suffices. Extrapolation to zero thickness is then extremely accurate. A rough estimation of the number of secondaries emitted above the (n,2n) threshold can be made from total multiplication measurements in thin and thick shells. If the total leakage of neutrons above the (n,2n) threshold is also measured, then the effective number of the secondaries above the (n,2n)-threshold can be directly determined for each shell thickness. Finally the model developed is used in section V to analyse Takahashi's /3/ measured multiplications in Pb shells.

I. Theory

We start with a monoenergetic problem. D-T neutrons are generated at the "source energy", enter the amplifier body and have a chance for making one or more collisions. The probability for a collision depends on the spatial distribution of the collisions and on the angular distribution of the neutrons coming out of these collisions. The calculation of an average probability for a collision becomes simpler if the angular distribution is assumed isotropic, so that preceding collisions can be assumed to constitute an isotropic collision source. Such an assumption is known to be quite accurate, provided the neutrons generating the collision source are considered to have interacted with the medium with a reduced total cross section, the so-called transport cross section

$$\sigma_{tr} = \sigma_t - \mu\sigma_{e1} \quad (I.1)$$

As a consequence, the average collision probabilities are functions of Σ_{tr} , the macroscopic transport cross section. We shall denote the average collision probability of the source neutron by P , and the average probabilities for subsequent collisions by W_1, W_2 , etc.

Two kinds of secondaries, emitted in a collision, are considered:

λ = the number of secondaries produced in a collision
below B_2 , the (n,2n) threshold

η = the number of secondaries produced in a collision
above B_2 * (I.2)

$\nu = \lambda + \eta$, the total number of secondaries produced
in a collision

* Actually we mean "in the source group" instead of "above B_2 ", but we use the latter term in the interest of an overall consistency in the article.

In parallel we define some neutronic properties of the amplifying medium as follows:

L = the number of neutrons slowing down below B_2 per one source neutron

H = the number of neutrons leaking out of the amplifier above B_2 , per one source neutron (I.3)

M = L+H, the total multiplication of one source neutron

Good amplifiers have very small absorption cross sections, so H above B_2 is a measure of the total leakage out of the amplifier up to considerable amplifiers thicknesses. L is the number of neutrons leaking out or getting absorbed below B_2 . We shall return to the difference between M and the total leakage as we discuss later the analysis of experiments.

In order to relate L, H, M, to λ, η, ν we introduce also

F = the total number of collisions above B_2 , resulting from the introduction of one source neutron into the medium (I.4)

clearly $F = P + P\eta W_1 + P\eta W_1\eta W_2 + \dots$ or,

$$F = P \cdot (1 + \eta W_1 + \eta^2 W_1 W_2 + \eta^3 W_1 W_2 W_3 + \dots) \quad (I.5)$$

Since we are not considering amplifiers which are supercritical above B_2 , i.e. $\eta < 1$, the sum in Eq.(I.5) converges. At each collision λ neutrons fall below B_2 , hence

$$L = \lambda F \quad (I.6)$$

Also, at each collision extra $\nu-1$ neutrons are added to the medium, hence

$$M = 1 + (\lambda + \eta - 1)F \quad (I.7)$$

then Eqs. (I.3), (I.5), (I.7) together give

$$H = 1 - (1 - \eta)F \quad (I.8)$$

Obviously we would like to find a practical approximation for the infinite sum in F, Eq. (I.5). It has been shown ^{/8/} that, whatever the initial collision source, namely the source for W_1 , the series W_1, W_2 , rapidly converges to a "stationary" W_m , the source which is distributed like a reactor fundamental mode flux ^{/9/}. Often W_3 is already practically coincident with W_m . A first order approximation to the sum in F then results from equating

$$W_1 = W_2 = \dots = W_m \quad (I.9)$$

which immediately yields

$$F = P \frac{1}{1 - \eta W_m} \quad (I.10)$$

Often, see e.g. later for a central source in a spherical shell, W_1 is an average over a collision source which is still distributed differently from the stationary distribution, therefore it is necessary to define

$$W_1 = W_m + \delta \quad (I.11)$$

with the result

$$F = P (1 + (W_m + \delta)\eta + (W_m + \delta)W_m\eta^2 + (W_m + \delta)W_m^2\eta^3 + \dots) \quad (I.12)$$

and, after summation,

$$F = P \cdot \frac{1 + \eta(W_1 - W_m)}{1 - \eta W_m} \quad (I.13)$$

In many instances the term $\eta(W_1 - W_m)$ is small and may be brought into the denominator, with the approximate result

$$F \sim P \frac{1}{1 - \eta W_1} \quad (I.14)$$

Next, we show that if W_m is approached from above by the series W_1, W_2, \dots (this will be the case for a spherical shell), then the expression of

Eq.(I.14) for F is a valid approximation even if the term $\eta(W_1 - W_m)$ is not very small. If generally

$$W_n = (1 + \rho_n) W_m \quad n = 1, 2, \dots, \quad (I.15)$$

it follows:

$$F = P(1 + (1 + \rho_1)W_m \eta + (1 + \rho_1)(1 + \rho_2)W_m^2 \eta^2 + \dots), \quad (I.16)$$

where it is assumed that

$$\rho_1 > \rho_2 > \rho_3 > \dots > 0 \quad (I.17)$$

We do not know the actual values of ρ_i , but we certainly can make a choice of ρ_i consistent with (I.17). We choose

$$\rho_n = \frac{\rho_1^n}{\prod_{k=1}^{n-1} (1 + \rho_k)} \quad (n = 2, 3, \dots) \quad (I.18)$$

It is easy to show by induction that

$$\prod_{k=1}^n (1 + \rho_k) = 1 + \sum_{k=1}^n \rho_1^k \quad (I.19)$$

from which

$$F = P (1 + (1 + \rho_1)W_m \eta + (1 + \rho_1 + \rho_1^2)(W_m \eta)^2 + \dots) \quad (I.20)$$

Regrouping the summations in Eq.(I.20) yields

$$F = P \left[(1 + W_m \eta + W_m^2 \eta^2 + \dots + \rho_1 W_m \eta (1 + W_m \eta + W_m^2 \eta^2 + \dots) + \rho_1^2 (W_m \eta)^2 (1 + W_m \eta + W_m^2 \eta^2 + \dots)] \quad (I.21)$$

therefore

$$F = P \frac{1}{(1-W_m \eta)(1-\rho_1 W_m \eta)} \quad (I.22)$$

and with ρ_1 as defined in Eq.(I.15), finally

$$F = P \frac{1}{1-W_1 \eta} \quad (I.23)$$

In order to simplify the notation, we define $W \equiv W_1$ and rewrite Eq.(I.23) as

$$F = P \frac{1}{1-W\eta} \quad (I.24)$$

a result stating that the total collision rate generated above B_2 is as if all generations of non-source neutrons were colliding with the average probability of the first generation.

The calculation of the collision probabilities P and W will be discussed in the next section, and the case of neutron multiplication with energy degradation will be taken up later, but Eqs.(I.6), (I.8) and (I.24) already constitute an approximate formulation of the amplification in high and medium mass number materials. In these materials at 14 MeV, the $(n,2n)$, $(n,3n)$ and (n,f) events for 14 MeV source neutrons produce neutrons almost entirely below B_2 , i.e., below the multiplication range; inelastic events which do produce neutrons in the multiplication range are a small fraction of the total of all events; and elastic scattering leaves most of the scattered neutrons in the source group. Since the inelastic events are relatively few we may "enforce" a one-group process by assigning a fraction f of the inelastically scattered neutrons to stay in the source-group, $1-f_1$ to fall below the multiplication range. Thus,

$$\eta \sim \frac{\sigma_{eltr} + f_1 \sigma_{inelastic}}{\sigma_{tr}} \quad (I.25)$$

$$\lambda \sim \frac{(1-f_1) \sigma_{inelastic} + 2\sigma_{n,2n} + 3\sigma_{n,3n} + v_f \sigma_{n,f}}{\sigma_{tr}}$$

(for high and medium mass number elements)

We note that Eqs.(I.6), (I.7), and (I.8) entail

$$\frac{L}{\lambda} = \frac{M-1}{\nu-1} = \frac{1-H}{1-\eta} \quad (\text{I.26})$$

Eq.(I.26) is thus characteristic of the one-group amplification process. If M and H are measured, or calculated with a multigroup transport code, then the validity of the simple one-group scheme can be tested by forming the ratios L/λ , $(M-1)/(\nu-1)$, $(1-H)/(1-\eta)$.

Turning next to the degradation process, we start by rewriting Eq.(I.24) as

$$\frac{F}{P} = 1 + \frac{\eta W}{1-\eta W} \quad (\text{I.27})$$

If no source-group neutrons were generated in the collisions, i.e., $\eta=0$, then the total collision count per collision of source neutrons would remain 1. If $\eta \neq 0$, then a collision of source neutrons introduces η neutrons into the system and $\eta W/(1-\eta W)$ is the total collision count generated by this η "collision source". Generally, we may consider the collision events started by non-source neutrons in dissociation from the actual source by starting with a distributed source of neutrons. If we define

$$\psi(\eta, W) = \text{the total collision count generated from 1 distributed neutron by collisions characterized by an } \eta \text{ neutron-return per collision, and by an average probability } W \quad (\text{I.28})$$

then, starting with ζ distributed neutrons, from balancing it follows:

$$\psi = W(\zeta + \eta\psi) \quad (\text{I.29})$$

The bracketed sum on the R.H.S. of Eq.(I.29) is the total number of neutrons produced directly as source neutrons (ζ) or by collisions ($\eta\psi$). The total collision rate of these neutrons is their number multiplied by the collision probability W , and the product is equated to the L.H.S. of the equation.

Eq.(I.29) is a finite-medium counterpart of the infinite medium balance equation which is clearly $\psi = \zeta + \eta\psi$. The solution of Eq.(I.29) is

$$\psi = \frac{\zeta W}{1 - \eta W} \quad (\text{I.30})$$

which, expectedly, reduces to the second term of the R.H.S. of Eq.(I.27) for the case $\zeta = \eta$.

We generalize Eq.(I.29) to the energy-dependent case by introducing a multi-group picture. But the results from the following analysis can also be concluded in a continuous energy degradation description. We assume a total number of G energy groups, counting from source to the $(n, 2n)$ threshold energies. The problem is characterized by

ζ_n , ($n=1, G$) = number of distributed-source neutrons in group n

ν_{kn} , ($k=1, n(n=1, G)$) = number of neutrons produced in group n by a collision in group k

W_n = an average collision probability in group n . for all generations of collisions (I.31)

ψ_n = the total collision count generated in group n

We have to note that a-priori it is not certain that in the energy dependent problem an average W_n can be found which well approximates the average collision probability of all collision generations; secondly the explicit definition of such a W_n in geometry and cross section terms may be difficult compared to the single group case. Both these questions will be taken up in the next section. For the moment we borrow the later conclusion that, for a bare homogeneous body, in diffusion theory an approximation to W_n can be found.

The multigroup generalization of Eq.(I.29) is

$$\psi_n = W_n \left(\zeta_n + \sum_{k=1}^n \psi_k \nu_{kn} \right) \quad (\text{I.32})$$

We divide by W_n and sum up over all groups

$$\sum_{n=1}^G \frac{\psi_n}{W_n} = \sum_{n=1}^G \zeta_n + \sum_{n=1}^G \sum_{k=1}^n \psi_k \nu_{kn} \quad (\text{I.33})$$

Rearranging the double sum, we have:

$$\sum_{n=1}^G \frac{\psi_n}{W_n} = \sum_{n=1}^G \zeta_n + \sum_{k=1}^G \psi_k \left(\sum_{n=k}^G v_{kn} \right) \quad (\text{I.34})$$

Define:

$$\psi \equiv \sum_{k=1}^G \psi_k, \quad \text{the total collision rate in the amplification range} \quad (\text{I.35})$$

$$W \equiv \frac{\psi}{\sum_{n=1}^G \frac{\psi_n}{W_n}} \quad \text{the average collision probability for the amplification range} \quad (\text{I.36})$$

$$\zeta \equiv \sum_{n=1}^G \zeta_n, \quad \text{the total distributed collision-source in the amplification range} \quad (\text{I.37})$$

$$\eta_k \equiv \sum_{n=k}^G v_{kn}, \quad \text{the total number of neutrons produced in group } k \text{ in the amplification range} \quad (\text{I.38})$$

$$\eta \equiv \frac{\sum_{k=1}^G \eta_k \psi_k}{\psi} \quad \text{the average number of neutrons produced in the amplification range.} \quad (\text{I.39})$$

Then Eq.(I.34) reads

$$\psi = W(\zeta + \eta\psi), \quad (\text{I.40})$$

which has exactly the same form as Eq.(I.29). The interpretation of Eq.(I.40) is as follows. If W is a properly defined average collision probability over the amplification range (Eq.(I.36)), then a distributed collision-source of ζ neutrons in this range will generate a total collision count as if the collision process was a one-group process, each collision generating η (Eq.I.39) neutrons back into the group.

Obviously, if also

$$\lambda_n = \text{the number of neutrons produced in a collision} \quad (I.41)$$

$$\text{in group } n \text{ below the amplification range,}$$

then,

$$\lambda \equiv \frac{\sum_{n=1}^G \lambda_n \psi_n}{\psi} \text{ is the average number of neutrons produced} \quad (I.42)$$

$$\text{below the amplification range by collisions in the}$$

$$\text{amplification range}$$

η and λ characterize the amplification of non-source neutrons. As such they must be independent of ζ , the distributed collision-source strength.

Indeed the solution of Eq. (I.40) is

$$\psi = \zeta \frac{W}{1-\eta W} \quad (I.43)$$

Together with Eqs. (I.39) and (I.42), the nondependence of λ and η on the magnitude of ζ can be ascertained. We make use of this fact by choosing

$$\zeta = \eta \quad (I.44)$$

in order to ensure that, as of the first emission of non-source neutrons, the number emitted into the amplification range is the correct average number by which the effective one-group description for non-source neutrons is enabled.

With this choice

$$\psi = \frac{\eta W}{1-\eta W} \quad (I.45)$$

and the collision rate of non-source neutrons is entirely specified.

In similarity to Eqs. (I.6) and (I.8), the leakage and slowing down rates for one non-source neutron, H^* and L^* respectively, are given by (W replaces P)

$$\left. \begin{aligned} H^* &= \frac{1-W}{1-\eta W} \\ L^* &= \frac{\lambda W}{1-\eta W} \end{aligned} \right\} \text{(per one non-source neutron)} \quad (I.46)$$

The total counts, per one source neutron, are

$$\begin{aligned} H &= 1 - P + P\eta H^* \\ L &= P\lambda_{\text{source}} + P\eta L^* \end{aligned} \tag{I.47}$$

or,

$$H = 1 - \frac{(1-\eta^{\text{eff}})P}{1-\eta^{\text{eff}}W} \tag{I.48}$$

$$L = \lambda^{\text{eff}} \frac{P}{1-\eta^{\text{eff}}W}$$

where

$$\eta^{\text{eff}} \equiv \eta \tag{I.49}$$

$$\lambda^{\text{eff}} \equiv \lambda_{\text{source}} + (\lambda - \lambda_{\text{source}})\eta W$$

Eqs.(I.48) and (I.49) constitute the main result of the energy degradation analysis. In form they are identical with the one-group Eqs.(I.6) and (I.8), however η^{eff} and λ^{eff} are now parameters including the effect of the degradation in the amplification range. We observe that, if there is a considerable variation of $\eta(E)$ with energy, then η^{eff} may be considerably different from η_{source} (i.e. from η of the 1st (source) group), depending through the collision rate energy spectrum (solution of Eq.I.32) on the size of the amplifier. Variation in λ^{eff} , in comparison with λ_{source} , are more restrained due to the factor ηW multiplying the difference $(\lambda - \lambda_{\text{source}})$ in Eqs.(I.4a). In principle, though, there is a dependence of λ^{eff} and η^{eff} on the size of the system, or equivalently on the average W . Thus

$$\begin{aligned} \lambda^{\text{eff}} &= \lambda^{\text{eff}}(W) \\ \eta^{\text{eff}} &= \eta^{\text{eff}}(W) \end{aligned} \tag{I.50}$$

Fortunately, as will be shown in section III, often this dependence is weak, enabling the formation of size-dependent λ^{eff} and η^{eff} to go with the Eqs.(I.48) namely the effective one-group equations for the amplification process.

II. Collision Probabilities

We begin again with the monoenergetic one-group problem.

Collision probabilities can be calculated by transport or Monte Carlo methods for a given geometry. Much simplicity, and some physics insight, is gained from the pursuit of analytical expressions for collision probabilities. We shall first deal in general with the collision probabilities involved in the theoretical formulae of section I, then the discussion will focus entirely on spherical shells; most attention will be given to W_m .

As discussed before, an exact evaluation of P is of utmost importance.

If the source-body has a one-dimensional symmetry, then

$$P = 1 - e^{-N\sigma_{tr}\Delta} \quad \text{II.1}$$

where Δ is the body thickness in the direction connecting the source and the body. In other cases averages must be performed

$$P = 1 - \langle e^{-N\sigma_{tr}\Delta} \rangle \quad \text{II.2}$$

While there is a great variety in P , depending on the shape of the body and the source-body, there are common features in W_m . It has been demonstrated^{/8/} that, whatever the distribution of an external source or of the first collided neutrons is, the distributions of neutrons with higher collisions rapidly converges to an asymptotic form ϕ_m . Bethe^{/7/} has argued that ϕ_m for a bare body is exactly the fundamental-mode flux distribution for the body at criticality in the group of neutrons under consideration. The central argument is that the n^{th} distribution depends on the $(n-1)^{\text{th}}$ distribution but not on the number of neutrons generated in the $(n-1)^{\text{th}}$ collision. Therefore one may choose the number of neutrons emitted back into the colliding group, namely η , to be of an appropriate magnitude such that in the limit of large n the total number of neutrons making the n^{th} and $(n+1)^{\text{th}}$ collisions is the same. Then the body is critical and the spatial distribution of the neutrons is the fundamental mode flux distribution.

Within the diffusion approximation a basic relation between the collision probability W_m and the geometrical buckling of the critical system can be established. Assuming a one-group neutron population, in each collision $\tilde{\eta}$ neutrons are emitted back in the group and $\tilde{\lambda}$ neutrons below the group. The number $\tilde{\eta}$ was so adjusted as to ensure criticality by these one-group neutrons, and $\tilde{\lambda}$ is essentially an absorption fraction, since this is the number of neutrons disappearing from the group on each collision. The group does of course not contain source neutrons; the effective one-group leakage and absorption (slowing down) are given by H^* and L^* of Eqs.(I.46). Define:

$$P_{\text{non}} \equiv \text{the non-leakage probability from a critical bare reactor} \quad (\text{II.3})$$

Since neutrons either leak out or are absorbed in a one-group picture, the non leakage probability is

$$P_{\text{non}} = \frac{L^*}{L^*+H^*} = \frac{\lambda W_m}{\lambda W_m + (1-W_m)} \quad (\text{II.4})$$

and since

$$\lambda = \frac{\Sigma_a}{\Sigma_{\text{tr}}}, \quad (\text{II.5})$$

where Σ_a is the absorption cross section, it is

$$P_{\text{non}} = \frac{1}{1 + \left(\frac{1-W_m}{W_m}\right) \frac{\Sigma_{\text{tr}}}{\Sigma_a}}, \quad (\text{II.6})$$

On the other hand, the diffusion theory expression for the non leakage probability out of a critical bare reactor is

$$P_{\text{non}} = \frac{1}{1 + \left(\frac{D}{\Sigma_a}\right) B^2}, \quad (\text{II.7})$$

where D is the diffusion coefficient, and B^2 the geometrical buckling. Comparing (II.6) with (II.7), we obtain a basic relation

$$W_m = \frac{\Sigma_{\text{tr}}}{\Sigma_{\text{tr}} + DB^2} \quad (\text{II.8})$$

with

$$D = 1/(3\Sigma_{tr}) , \text{ also}$$

$$(1-W_m)^{-1} = 1 + 3\left(\frac{\Sigma_{tr}}{B}\right)^2 . \quad (\text{II.9})$$

For all bodies of usual interest, such as spheres and spherical shells, finite and infinite slabs, finite and infinite cylinders, B^2 is an eigenvalue of the wave equation $\nabla^2\phi + B^2\phi = 0$ and is given by

$$B^2 = \sum_{i=1}^I B_i^2 \quad (I=1, \text{ or } 2, \text{ or } 3) \quad (\text{II.10})$$

where I is the order of dimension of the geometry. The diffusion boundary conditions also determine the partial bucklings B_i as

$$B_i^2 = \frac{C_i^2}{(\Delta_i + d)^2} \quad (\text{II.11})$$

where C_i are constants, typical of the curvature in the i^{th} dimension, Δ_i is the body extension along the i^{th} dimension, and d is the extrapolation distance. Then

$$3\left(\frac{\Sigma_{tr}}{B_i}\right)^2 = \frac{(x_i + \delta)^2}{C_i^2} \quad (\text{II.12})$$

where $x_i = \Sigma_{tr} \Delta_i$, the optical thickness in the i^{th} dimension, and δ is the extrapolation distance in units of the mean free path.

Introducing the optical mean chord length ℓ as a representative measure of the body size, we have

$$x_i = \rho_i \ell \quad (\text{II.13})$$

and

$$(1-W_m)^{-1} = 1 + 3 \sum_i \left(\frac{\rho_i}{C_i}\right)^2 \left(\ell + \frac{\delta}{\rho_i}\right)^2 \quad (\text{II.14})$$

In diffusion approximation we have to assume that the body is sufficiently large in each direction. Thus $\delta \ll x_i$, or $\delta / \rho_i \ll \ell$, and with the expansion of squares in Eq.(II.14) in two terms, finally

$$(1-W_m)^{-1} = 1 + \epsilon_1 \ell + \epsilon_2 \ell^2 . \quad (\text{II.15})$$

Eq.(II.15) is not new. Kumar ^{/9/} has fitted ϵ_1 and ϵ_2 for bodies of various shapes not only in the diffusion range $\ell \gg 1$, but also down to zero chord length. In Table (II.1) we compare Kumar's values for ϵ_2 in the ranges (0-3) and (1-10) for ℓ , with the diffusion theory ϵ_2 value for $\ell \gg 1$.

We turn our attention next to spherical shells with a central point source. P is exactly given by Eq.(II.1). In order to find suitable expressions for W, we have utilized tables and graphs given by Bethe et al ^{/7/} for W and W_m in the optical thickness range $0 < x \leq 1.6$.

We start with the conjecture that W_m can be fitted by the form of Eq.(II.15) Rewriting Eq.(II.15) as

$$\frac{W_m(k, x)}{(1-W_m(k, x))x} = \alpha_k + \beta_k x \tag{II.16}$$

where

$$\begin{aligned} x &\equiv \Sigma_{tr} (R_2 - R_1) \\ k &\equiv R_1 / R_2 \end{aligned} \tag{II.17}$$

a fitting of the L.H.S. of Eq.(II.16) by the R.H.S. was carried out for each k. For k=0, .2, .4., .6 and .8 the L.H.S. was an almost perfect straight line in x in the range (0. -1.6), with some relatively small magnitude exceptions at $x \leq 0.2$. For k=1.0 (the limit of an infinitely narrow shell), there is some deviation of the $W_m / \{(1-W_m)x\}$ value from a straight line. These fits are shown in Figs. II.1 through II.6. The α_k and β_k , determined by this procedure, are given in Table II.2.

The curve $W(k, x) / \{(1-W_m)x\}$ is above a straight line, the deviation increasing with x. An example of this characteristics feature is shown in Fig. II.1. We therefore tried to fit W by adding a third, square, term to the R.H.S. of Eq.(II.6), namely

$$\frac{W(k, x)}{(1-W(k, x))x} = \alpha_k + \beta_k x + \gamma_k x^2, \tag{II.18}$$

retaining the α_k and β_k from the fit of Eq.(II.16). The fitting of the γ_k values are also given in Table II.2. Table II.3 shows a comparison between accurate W(k, x)

values, and values obtained with Eq.(II.18) and the parameters of Table II.2. Most W values are reproduced to better than 1%, with some exceptions for $k=0$ at low x values.

For large x values we turn to Eq.(II.9). As x becomes larger than 1, an exact fit for α_k becomes less important; therefore our interest in Eq.(II.9) focusses on obtaining from it β_k values. The general solution of the wave equation in spherical geometry can be represented by^{/7/}

$$\phi = \frac{\sin B(r+\delta)}{r} \quad (II.19)$$

Setting ϕ' to zero at the inner radius R_1 , and setting ϕ to zero at the extrapolated boundary R_2+d leads to

$$B(\Delta+d) = \pi - \tan^{-1}\left(\frac{k}{1-k} \cdot B\Delta\right) \quad (II.20)$$

To determine β_k , the limit $\Delta \rightarrow \infty$ is investigated, therefore $d/\Delta \rightarrow 0$, thereupon rendering Eq.(II.20) an expression for $B\Delta$. But we shall also touch upon the solution of Eq.(II.20) for finite x , therefore we write down the transport relation between Bd and $B\Delta$ at criticality^{/7/}, namely

$$Bd = 0.7 \tan^{-1} \frac{B\Delta}{x} \quad (II.21)$$

Having solved the coupled equations (II.20) and (II.21) for a selection of x values from zero to infinity we observed that

$$B(\Delta+d) = C(x) \quad (II.22)$$

where $C(x)$ is a weak function of x . Values $\beta(\infty)$, $\beta^*(1)$, $\beta^*(0)$, as determined from Eq.(II.22) and Eq.(II.9), are shown in Fig.II.4. Although the application of the diffusion theory relation, Eq.(II.9), is not strict for $x=0$ or $x=1$, we observe nevertheless the interesting fact that $\beta_k^*(0)$ are very close to the fitted β_k of Table II.2, except for the $k=1$ shell. We have no satisfactory argument for explaining whether this is merely a coincidence.

$\beta_k(\infty)$ are slightly higher than $\beta_k(0)$, repeating the pattern of Table II.1. (there, ϵ_2). We have had no numerical data to determine an optimal x , above which $\beta_k(\infty)$ should be used. The educated guess is $x = 3$, and results of the next two sections do not suggest any gross error in this choice. α_k and γ_k were kept the same for all x .

Next we examine the definition and application of collision probabilities in the slowing down context. P is a probability for source neutrons and is not affected by the slowing down process. As regards W , the question is whether its definition as in section I, and its dependence on Σ_{tr} , as above, hold. We have no way of directly examining this question, but we can examine instead the case of W_m .

The fundamental reactor theorem states that in the diffusion approximation the flux in the bare reactor is separated in space and energy, the spatial separant satisfying the same equation and boundary conditions as in the one-group case. Defining

$$\phi_g = f_g \psi(B) \quad \text{the fundamental mode flux in group } g \quad (\text{II.23})$$

and multiplying the wave equation for $\psi(B)$ by f_g we obtain

$$\nabla^2 \phi_g \times B^2 \phi_g = 0 \quad (\text{II.24})$$

The total leakage and absorption in group g are

$$\begin{aligned} \text{Leakage in group } g &= -\int dV (\nabla \cdot \underline{J}_g) \\ \text{Absorption in group } g &= \int dV \Sigma_{a,g} \phi_g \end{aligned} \quad (\text{II.25})$$

The multigroup relation between current (\underline{J}_g) and flux (ϕ_g) is strictly not given by Fick's law as in one-group diffusion, but we may assume that the slowing down problem has been solved and that an effective $\Sigma_{tr,g}$ has been determined such that the current and flux are related by

$$\underline{J}_g = - \frac{1}{3 \tilde{\Sigma}_{tr,g}} \cdot \phi_g \quad (\text{II.26})$$

The non-leakage probability in group g is then

$$P_{\text{non},g} = \frac{(\text{Absorption})_g}{(\text{Absorption})_g + (\text{Leakage})_g} = \frac{1}{1 + \frac{B^2}{3 \tilde{\Sigma}_{tr,g} \Sigma_{a,g}}} \quad (\text{II.27})$$

Comparing Eqs-(II.27) and (II.28) yields

$$(1 - W_{m,g})^{-1} = 1 + 3 \frac{\tilde{\Sigma}_{tr,g} \Sigma_{tr,g}}{B^2} \quad (II.29)$$

Generally $\tilde{\Sigma}_{tr,g} \neq \Sigma_{tr,g}$, but if we simplify

$$\tilde{\Sigma}_{tr,g} \sim \Sigma_{tr,g}, \quad (II.30)$$

then we have a formal analogy between Eq.(II.29) and the one-group expression for W_m , Eq.(II.9). If one wants to estimate the corresponding error (usually small, for a moderate variation of $\sigma_{tr}(E)$ in the multiplication range) inherent in Eq.(II.30), then there is also a practical analogy between Eq.(II.29) and Eq.(II.9). Practically, then $W_{m,g}$ can be evaluated from Eq.(II.16) and Table II.2 in the same way as W_m . As regards $W_{1,g}$ we conclude the same, conjecturing that the difference $W_{m,g} - W_{1,g}$ remains as small as the one-group difference $W_m - W_1$.

Finally we have to remember that the analysis offered above was based on diffusion theory and is applicable with increasing validity to increasing amplifier sizes. The reverse is true as we decrease the size of the amplifier. The energy spectra based on the solution of the generalized slowing down equations (I.32), with W_m derived by the method discussed above, will deviate to some extent from the true spectra as the system becomes smaller.

III. Analysis of the Neutron Amplification in Pb,Zr,Cu,Fe, U238 and Be

The theory laid out in the preceding two sections was applied to Pb,Zr, Cu,Fe, U238 and Be. A D-T neutron source was assumed at the center of a series of spherical shells for each of these materials. All shells had an inner radius of 10 cm, and the shell thicknesses ranged from 0.2 to 50 cm. The transport code ITRAN, with ENDF/B-IV cross sections for these materials, was used to calculate the multiplicities L, H, and M.

The analysis in this section will show that λ^{eff} and η^{eff} for the amplification energy ranges of these materials have a smooth dependence on the size of the shell, or on W, so that the amplification process in these materials can be accurately described with geometry independent one-group parameters, or two-group cross sections for Be.

Characteristic data which are relevant to neutron amplification in the materials, mentioned above, are summarized in Tables III.1. In each material the relevant B_2 , the (n,2n) threshold, was taken to be some cut-off energy below which $\sigma_{n,2n}$ is negligible. Effective one-group cross sections are given in Table III.2. The comparison between the L,H,M values predicted with the one-group description and the ITRAN results, is shown in Tables III.3.

We use the term "one-group" in the following sense. The equations determining L and H ($M=L+H$) are Eq.(I.48), with two exceptions: for U238 they are modified to account for the amplification by fission below the (n,2n) threshold; for Be a two-group process is taken. In these equations P is calculated from Eq.(II.1) with a correction applied to the shell thickness Δ , to account for the fact that the source in the ITRAN calculations, for numerical reasons, was not a centerpoint but rather a distributed source in a small shell around the centerpoint. The correction is derived in an appendix. W, the average collision probability for once-collided neutrons, is given by Eq.(II.18). The parameters $\alpha_k, \beta_k, \gamma_k$ for this equation were interpolated from entries in Table II.2. The σ_{tr} value for which W was calculated ($x=\Delta\Sigma_{\text{tr}}$), was σ_{tr} for the source group.

The terms η_{el} and ζ_g in the data tables mean, respectively, $\sigma_{eltr}/\sigma_{tr}$ and $\sigma_{l \rightarrow g}/\sigma_{tr,1}$. As we consider the data for Pb, Zr, Fe, and Cu we notice that in all these materials (a) η is small, (b) σ_{tr} is slightly increasing in the energy direction from the source energy to B_2 . These trends are helpful in setting up an η^{eff} , as can be realized from the form of Eqs(I.48). Strictly, $W^{eff}(\Delta)$ should be determined from the solution of the slowing down equations (I.32), then from Eq.(I.36). Because of the increasing σ_{tr} (see (b) above) it is,

$$W^{eff}(\Delta) > W(\Delta\Sigma_{tr,1}) . \quad (III.1)$$

With small η 's the exact W^{eff} value in small shells is unimportant and an η^{eff} can be chosen so as to compensate in the thick shells for the fact that in the one-group model one sets $W^{eff} = W(\Delta\Sigma_{tr,1})$. Tables III.3 show that the one-group parameters for Pb, Zr, Cu, and Fe of Table III.2 indeed reproduce very accurately the L,H, and M multiplicities as calculated with ITRAN and ENDFB/B-IV.

In U238 the neutrons slowed down below B_2 are further amplified because the fission threshold of U238, ~ 1 MeV is lower than the (n,2n) threshold, i.e. ~ 6 MeV. However, we may estimate this further amplification from the observation that in a heavy element the neutrons which fall below B_2 almost entirely are scattered inelastically, the spectrum being of the evaporative type.

We also observe that the evaporative-type spectra of secondaries from (n,2n) and (n,3n) reactions are, in gross terms, not much different from a fission spectrum. Approximately, then, all neutrons generated in U238 by collisions above B_2 are generated with a fission spectrum. Hence we may utilize the reactor theory notion of the fast effect to estimate the amplification of neutrons fallen below B_2 . For each neutron borne with a fission spectrum, the fast-effect factor ϵ is the number of neutrons degraded below the fission threshold, either by direct collisions in the fuel or by leaking into a non-returning moderator. Presently L is the number of neutrons appearing below B_2 in a fission spectrum; hence ϵL is the count of all neutrons either leaking out in the energy range between the fission and (n,2n) threshold or slowing down below the fission threshold. Eventually all neutrons below the fission threshold either leak out or get absorbed ; therefore, in other words

ϵL is the number of neutrons leaking out below B_2 or which are absorbed below the fission threshold.

Following the considerations above we generalize our definitions of H, L, M to read

$$\begin{aligned} H &\equiv \text{total leakage above the } (n,2n) \text{ threshold} \\ \epsilon L &\equiv \text{total leakage below the } (n,2n) \text{ threshold} \\ &\quad \text{and absorption below the fission threshold} \\ M &\equiv H + \epsilon L \end{aligned} \tag{III.2}$$

From reactor theory, an expression for ϵ is /8/

$$\epsilon = 1 + \frac{0.09P_1}{1-0.52P_2} \tag{III.3}$$

where P_1 is the collision probability for fission-generated neutrons, and the probabilities for subsequent collisions above the fission threshold are assumed to be all equal to P_2 , the probability for second collisions. In our case, P_1 is equal to W , the average collision probability following the collision of the source neutrons, therefore W_m is approached from above and, due to the analysis of section I, the best estimate for ϵ would be by

$$\epsilon = 1 + \frac{0.09W}{1-0.52W} \tag{III.4}$$

In order that Eq.(III.4) can effectively be used in Eqs.(III.2), then in the one-group Eqs.(I.48), we assume that W of Eq.(III.4) is $W(\Delta\Sigma_{tr,1})$, namely the same W as used in Eq.(I.48). This assumption rests on the observation that $\sigma_{tr}(E)$ in the range from the fission to the $(n,2n)$ threshold is only slightly higher than $\sigma_{tr}(E)$ in the range from the $(n,2n)$ threshold to source. The comparison of H, ϵL , M by Eqs.(I.48), (III.2), and (III.4) with the corresponding multiplicities by the ITRAN runs is shown in Table III.3.e. to be very satisfactory.

In Be, expectedly, the amplification is not possible in a one-group description. With very high η values, and an extensive energy range from source to B_2 , there are considerable changes in η^{eff} and λ^{eff} with the shell thickness.

These relatively marked changes are the result of energy spectrum shifts in the amplification range. In Fig. III.1, the spectrum of neutrons, $F(E)$, in the energy range 2-13 MeV for three Be shells of thicknesses 3, 9 and 50 cm is shown. We note that there is a good degree of agreement between the ITRAN produced spectra and the spectra evaluated by the solution of the generalized slowing down equations (I.32). In corroboration of the arguments developed at the end of section II we also note that the generalized slowing down spectra lose accuracy as the shell becomes thinner.

For the two-group description for Be we chose the first group to coincide with the 13.5 - 15.0 MeV range used as source group in the ITRAN calculations. The group parameters in the two-group description are

η_{11} - the actual number of neutrons generated in group 1 by collision in group 1.

ζ_1 - the actual number of neutrons generated in group 2 by collisions in group 1

λ_1 - an effective number of neutrons generated below B_2 by collisions in group 1

η_2 - an effective number of neutrons generated in group 2 by collisions in group 2

λ_2 - an effective number of neutrons generated below B_2 by collisions in group 2.

$\sigma_{tr,1}$ - the actual σ_{tr} in group 1

$\sigma_{tr,2}$ - an effective σ_{tr} in group 2

With these parameters, as defined, and the leakages and slowing down in the two groups counted, the result is

$$\begin{aligned}
 L &= \frac{P_1}{1-\eta_{11}W_1} \left[\lambda_1 + \zeta_1 \lambda_2 \quad \frac{W_2}{1-\eta_2 W_2} \right] \\
 H &= \frac{P_1}{1-\eta_1 W_1} \left[1 - \eta_1 - \zeta_1 \quad \frac{1-W_2}{1-\eta_2 W_2} \right]
 \end{aligned}
 \tag{III.5}$$

We emphasize that the choice of 13.5 MeV as the energy boundary between the two groups may not be optimal. The two-group Be parameters, as given in Table III.2 and used in Eqs.(III.5), leave some room for optimization, as can be judged from the comparison of the multiplicities for Be, namely Table III.3.f.

IV. The Role of the Theory in the Analysis of Multiplication Experiments

We shall begin with the simplest experiment, namely one designed to measure the total leakage K out of the shell:

$$K \equiv \text{measured total leakage out of the shell per one source neutron} \quad (\text{IV.1})$$

In order for the theory to be effective, we have to establish a practical relation between K and M. Obviously

$$M = K + A \quad (\text{IV.2})$$

$$A \equiv \text{absorption below the multiplication range per one source neutron} \quad (\text{IV.3})$$

If the experiments are performed in a range of thicknesses for which the absorption is negligible below the multiplication range, then $M \sim K$. If such is not the case, then A may be estimated by an iterative procedure, the nature of which will be discussed shortly. For the moment we go on assuming there is an effective way of determining $M(K)$.

The quantity easiest to determine from M is ν_{source} , the number of secondaries generated in a collision of source neutrons. In order to avoid the problem of multiple collisions one ideally performs the measurements in a number of thin shells and deduces ν from

$$\nu - 1 = \lim_{x \rightarrow 0} \frac{M-1}{P} \quad (\text{IV.4})$$

or, equivalently, one deduces $\sigma_{n,2n} + 2\sigma_{n,3n} - \sigma_a$ from

$$\sigma_{n,2n} + 2\sigma_{n,3n} - \sigma_a = \sigma_{\text{tr}} \left[\lim_{x \rightarrow 0} \frac{M-1}{P} \right], \quad (\text{IV.5})$$

the R.H.S of Eqs.(IV.4) and (IV.5) being the correct expressions for $\nu-1$ in the absence of multiple collisions. In Figs. IV.1, IV.2, and IV.3, we show such possible determinations of $\nu-1$ by extrapolation to zero thickness. We have used the ENDF/B-IV/ITRAN calculated multiplicities as "experimental" data. We have excluded from these Figs. the calculated data below 1 cm of thickness because of better simulating the non-ideal circumstances of the experiment. We observe that in all three Figs, for Pb, U238 and Be, the ν^*-1 values (we shall use ν^* for values determined by the R.H.S. of Eq.(IV.4) or of corresponding later expressions, prior to extrapolation to zero) constitute a steep curve as we approach zero. This renders the extrapolation to zero somewhat uncertain.

An improvement in the $\nu-1$ approach to zero may come as a result of assuming $\eta = \eta_{e1}$, where $\eta_{e1} = \sigma_{eltr} / \sigma_{tr}$, and utilizing the expression for $\nu-1$ as given by the present theory, namely

$$\nu-1 = \lim_{x \rightarrow 0} \frac{M-1}{P} (1-\eta W) \quad (IV.6)$$

We assume, of course, that $\sigma_{eltr}(E)$ and $\sigma_{tr}(E)$ are well known in the multiplication range so that some average $\langle \eta_{e1} \rangle$ can be used in Eq(IV.6). At least we assume that $(\eta_{e1})_{source}$ is known, and with this latter assumption we have evaluated the R.H.S. of Eq.(IV.6). We see (in Figs. IV.1, IV.2, IV.3) that the slope of ν^*-1 becomes much smaller for Pb and U238; the improvement in the ν^*-1 slope for Be is not so marked.

In itself, the fact that the slope of the ν^*-1 curve, as determined from Eq. (IV.6) remains high does not indicate that the procedure or the assumptions made are wrong. The fact may be that in Be $\eta \sim \eta_{e1}$ but that $\nu-1$ (i.e. $\sigma_{n,2n}$) increases rapidly with decreasing energy such that with the thickness of the shell, and the concurrent enhancement of the slowing down process, an increased ν^{eff} is being observed. We know that this is not a correct state of cross sections as we consult Table III.1.f; but as "experimenters" we have no access to such a table. But since our theory does take account of multiple collisions we may try to gain information about η from measurements in thick shells.

Suppose we consider η_{e1} as a zeroth estimate of η , namely $\eta^{(0)} = \eta_{e1}$, and that with this value for $\eta^{(0)}$ the ν value determined from thin-shells by Eq.(IV.6) is an $\nu^{(0)}$ value. Then, in order to utilize the thick-shell measurements, we invert the equation for M, Eq.(I.48), to read

$$\eta^{(1)} = \frac{1-P \frac{\nu^{(0)}-1}{M-1}}{W} \quad (IV.7)$$

thus obtaining an iterated value for η .

As we see in Table IV.1, a very reasonable η value for thick-shells is obtained by the iteration. Further the iterated η value is quite insensitive to $\nu^{(0)}-1$; this is important, because the $\nu-1$ value, determined from a steep ν^*-1 , may be in some error. Using the iterated η back in Eq.(IV.6), a much more convenient approach to zero is obtained for Be. In the case of Pb and U238 such iterations change very little because the assumption $\eta \sim \eta_{e1}$ for these materials happens to be a good $\eta^{(0)}$ estimate.

We have shown that the application of the theory to the experimentally determined quantity M assists in obtaining a convenient extrapolation to zero by which $\sigma_{n,2n}$ of source neutrons is determined. It also yields a rough estimate of η^{eff} (effective number of secondaries emitted into the multiplying range) for thick shells.

Returning to the problem of the absorption below B_2 , we suggest a solution by iteration. Let the procedure described above of determining a ν out of an M be formalized as an operation Q, thus

$$\nu = Q(M) \quad (IV.8)$$

and let the absorption below B_2 , as calculated by a transport code for a given ν , be denoted by

$$A = A(\nu) \quad (IV.9)$$

then the iteration process is prescribed by

$$\begin{aligned} \nu^{(0)} &= \nu \text{ as known initially} \\ M^{(n)} &= K + A(\nu^{(n)}) \\ \nu^{(n+1)} &= Q(M^{(n)}) \end{aligned} \quad (IV.10)$$

We continue with a measurement designed to determine the total multiplication M , as well as the leakage above B_2 , H . Since the theory makes a distinction between H and M , such a measurement could better make use of the theory than the sole determination of M . Inverting Eqs. (I.48) we have

$$\eta = \frac{P - (1-H)}{P - W(1-H)} \quad (IV.11)$$

$$\nu - 1 = (M-1) \frac{1-W}{P-W(1-H)}$$

Thus a direct determination of $\eta^{eff}(\Delta)$ and $\nu^{eff}(\Delta)$ from the measured $H(\Delta)$ and $M(\Delta)$ is possible. Figs. IV.1 through IV.4 show such directly-determined ν and η values, again the H and M values calculated with ITRAN/ENDF/B-IV, providing the "experimental" data. We have to keep in mind that W in Eqs. (IV.11) is a W^{eff} ; by its definition it depends on the cross section scattering matrix in the multiplication range, therefore there cannot be an unequivocal determination of η and ν through Eqs. (IV.11), from the measurement of just the two quantities M and H . Nevertheless, if the variation of σ_{tr} in the multiplication range is known, or sensible variations in W^{eff} can be estimated otherwise, bounds can be determined for the variation of $\eta^{eff}(\Delta)$ and $\nu^{eff}(\Delta)$. This already is some knowledge about the hardness of the spectrum of secondaries as a function of energy.

A measurement of M and H also requires the need to determine $M(K)$ by iteration. We assume that below the multiplication range cross section data are sufficiently accurate for the transport calculation of the absorption per one neutron slowing down below the multiplication range.

Define

$$\left(\frac{A}{L}\right)^{cal.} \equiv \text{the calculated absorption below } B_2 \text{ per one neutron introduced below } B_2 \quad (IV.12)$$

then, since,

$$M = K + \left(\frac{A}{L}\right)L \quad (IV.13)$$

we have

$$M = K + \left(\frac{A}{L}\right)^{cal.} (M-H) \quad (IV.14)$$

V. Analysis of Takahashi's Neutron Multiplication Experiments in Pb

Recent measurements by Takahashi et al^{/2/} show the multiplication in Pb to be much higher than calculated with current Pb cross section data. The following is an analysis of Takahashi's data, based on the presently developed theory.

The measurements were done for a D-T neutron source, placed in the center of a spherical cavity formed by Pb spherical shells. Four shells were measured, all four with the inner radius of 10 cm, and with thickness of 3,6,9, and 12 cm. The leakage spectrum of neutrons emerging from the shell was monitored and integrated above 0.2 MeV. These (0.2-14)MeV multiplications have to be multiplied by correction factors, determined by Takahashi through the use of transport calculations. Table V.1 shows the total multiplications.

Included in the table are also values of H. These were obtained by us from the experimental data. To be reminded, M-H is the multiplication below 7 MeV, the (n,2n) threshold; Takahashi reports experimental values for H_{.3}⁴, the multiplication in the range 0.3 to 4MeV. The difference H₄⁷ = H_{.3}⁷ - H_{.3}⁴ could be evaluated from a graph in the Takahashi article^{/2/}, showing the leakage spectrum per source neutron for the 9 cm shell. This is used, together with the ratios (H_{.3}⁷/H_{.3}⁴) as determined from ITRAN-ENDF/B-IV runs for all 4 shells, to form

$$(H_4^7)_{\text{shell}} = (H_{.3}^7)_{\text{SHELL}} \left[\frac{H_4^7}{H_{.3}^4} \right]_{\text{SHELL}}^{\text{TRAN}} \cdot \frac{\left[\frac{H_4^7}{H_{.3}^4} \right]_{\text{SHELL9}}^{\text{EXPER.}}}{\left[\frac{H_4^7}{H_{.3}^4} \right]_{\text{SHELL9}}^{\text{TRAN}}} \tag{V.1}$$

As can be seen in Table V.1, the (H₄⁷) values thus obtained are small fractions of the multiplications in the (0.3-4) MeV range. The approximation of Eq.(V.1) thus could not have introduced an appreciable error.

Table V.1 also shows the ratio ζ , namely

$$\zeta \equiv \frac{M-H}{M-1} \quad (V.2)$$

for the four shells, and it is noticed that ζ deviates only slightly across the four shells. According to Eq.(I.26), and the discussion following it, the constancy of ζ renders the one-group description of the multiplication a valid description.

In the preceding sections a one-group amplification process was described with the aid of two effective numbers, namely λ^{eff} and η^{eff} . Strictly, these numbers depend on the solution of the generalized slowing down equation (I.32) above $(n,2n)$ threshold, but adopting the strict approach means the use of the emission distribution data, the very data which should be determined from the experiment. Instead, we shall use a somewhat heuristic definition for the one-group parameters, not requiring an iterated solution of the slowing down equations.

Define

- σ - total transport cross section
- σ_e - elastic transport cross section
- σ_1 - inelastic cross section
- σ_2 - $(n,2n)$ cross section
- σ_3 - $(n,3n)$ cross section
- σ_a - absorption cross section
- f_1, f_2, f_3 - fractions of the neutrons emitted in, inelastic, $(n,2n), (n,3n)$ reactions respectively, which remain above B_2

The fractions f have to be regarded as effective fractions.

The neutrons are assumed to remain in the source-group during the collision process; certainly, for elastic scattering in Pb this is a valid assumption, but non-elastic neutrons falling below the source group bring about further multiplications only by a magnitude proportional to $\langle v-1 \rangle$, an average net multiplication over the emission spectrum. Thus,

$$f_i = \bar{f}_i \cdot \frac{\langle v-1 \rangle \text{ (over emission spectrum } i \text{ above } B_2)}{(v-1) \text{ at source energy}}$$

where

$$\overline{f}_i = \text{the actual fraction of neutrons emitted above } B_2 \quad (V.4)$$

by type i non-elastic collisions of source neutrons

We shall return later to consequence resulting from the distinction between the actual fraction \overline{f} and the effective fraction f . Next we analyse the experimental results, as summarized in Table (V.1) in terms of the cross sections and emission fractions as defined above. Neglecting σ_a from the start, we have 7 cross sections and fractions to consider, namely $\sigma, \sigma_1, \sigma_2, \sigma_3, f_1, f_2, f_3$. We can simplify by "disposing of" σ_3 with the definitions

$$\sigma_2^* = \sigma_2 + 2\sigma_3 \quad (V.5)$$

$$f_2^* = \frac{2f_2\sigma_2 + (1+3f_3)\cdot\sigma_3}{2\sigma_2 + 4\sigma_3}$$

These definitions are so set as to preserve the original definition of η and ν . They are now given by

$$\nu = 1 + \sigma_2^*/\sigma \quad (V.6)$$

$$\eta = 1 - [(1-f_1)\sigma_1/\sigma + (1-2f_2^*)\sigma_2^*/\sigma]$$

Since we have effectively a one-group process (Eq.(V.2), and the ensuing discussion), we write

$$\zeta = \frac{\nu-\eta}{\nu-1} = 2 - \left[2f_2^* - (1-f_1) \frac{\sigma_1}{\sigma_2^*} \right] \quad (V.7)$$

But, from Table V.1, $\zeta \sim 1.70$, therefore solving Eq.(V.7) for f_2^* yields

$$f_2^* = 0.15 + \frac{1}{2} (1-f_1) \frac{\sigma_1}{\sigma_2^*} \quad (V.8)$$

Suppose all inelastic neutrons remain non-degraded, then $f_1=1$, and $f_2^* = 0.15$. Clearly the effective return fraction of inelastic scattering may be smaller than 1, so we have

$$f_2^* \geq 0.15, \quad (V.9)$$

a very high, effectively non-degraded emission fraction of (n,2n) events.

The result of Eq.(V.9) is corroborated by the more direct approach of considering individual shell multiplications in Table (V.1) and trying to match them with a set of cross sections and emission fractions, as applied to the one-group amplification formulae (I.48), namely to

$$M-1 = (\nu-1) \frac{P}{1-\eta W} \quad (V.10)$$

There are 4 parameters in the expressions for ν and η of Eqs.(V.6). So to simplify we set $f_1 = 1$ (namely assume all inelastic events to be totally effective for re-amplification) from the start, in this way trying to obtain a low estimate for f_2^* . Now

$$M = M(\sigma, \sigma_2^*, f_2^*) \quad (V.11)$$

and the search is for the most fitting triad $(\sigma, \sigma_2^*, f_2^*)$.

Some results of the search are shown in Fig.V.1 through Fig.V.4. With $f_2^* = 0$, or $f_2^* = 0.1$, no triad could reproduce the experimental $M-1$ values with reasonable proximity. Only going as high as $f_2^* = 0.2$ resulted in marginal fitting. This value of f_2^* is consistent with the low limit for f_2^* given in Eq.(V.9) and found in a different manner.

We now turn to an interpretation of these f_2^* values in terms of f_2 and $\overline{f_2}$, namely the effective and actual (n,2n) secondary emissions returned for re-amplification. Eqs.(V.5) inverted reads

$$f_2 = f_2^* - \left[\frac{1}{2} - 2f_2^* \left(\frac{\sigma_3}{\sigma_2} \right) \right] \quad (V.12)$$

and defining,

$$m \equiv \frac{(\sigma_2 + 2\sigma_3) \text{ at } 14 \text{ MeV}}{\langle \sigma_2 + 2\sigma_3 \rangle \text{ for } (n,2n)+(n,3n) \text{ emissions above } B_2} \quad (V.13)$$

we have, by Eq.(V.3)

$$\overline{f_2} = mf_2^* - m \left(\frac{1}{2} - 2f_2^* \cdot \frac{\sigma_3}{\sigma_2} \right) \quad (V.14)$$

With B_2 of the isotopes of natural Pb being at least 6.7 MeV, the available energy left for the two emerging neutrons, after an (n,2n) collision at 14.7 MeV, is at most 8 MeV. The \bar{f}_2 fraction is then spread from 6.7 to 8 MeV, a small energy span just above B_2 . As a consequence, m is a large number. Current ENDF/B-IV data yield $m \sim 10$.

Fig. V.5 shows $\bar{f}_2 \cdot (\frac{\sigma_3}{\sigma_2})$ for four choices of (m, f_2^*) . The most probable line is the $(m=10, f_2^* = 0.2)$ line; as \bar{f}_2 goes from zero to the maximum possible value of 0.5, (σ_3/σ_2) goes from 2.0 to 1.5. As 14.7 is just 1.3 MeV above the minimum (n,3n) threshold of the isotopes of natural Pb, it is impossible that σ_3 has already risen so sharply at the expense of σ_2 . The least probable line is then $(m=5, f_2^* = 0.15)$ line: as f_2 goes from zero to 0.5, (σ_3/σ_2) goes from .75 to .25. Current data set σ_3/σ_2 at 0.015, nevertheless we could examine the .25 value for σ_3/σ_2 because for 14.7 MeV neutrons σ_3/σ_2 starts to become a steep increasing function of energy.

To assume $\sigma_3/\sigma_2 = 0.25$ results in $\bar{f}_2 = 0.5$. The latter implies that in each (n,2n) reaction one of the emerging neutrons takes up almost all of the available energy, namely 6.7 to 8 MeV. This should constitute a drastically different distribution of secondaries than the evaporation type spectrum with an average energy of ~ 3.5 MeV, as currently assumed for the two emission neutrons. We have, though, to rule out the former type of distribution as we study Fig.(V.6).

Fig. V.6 shows three spectra of neutrons in the range from 0.3 to 12 MeV. Neglecting the very low energy tail, this is the energy range for secondaries from nonelastic collisions. Of the three spectra, two are for the neutrons leaking out of the 9 cm shell: one was evaluated from a corresponding graph in the Takahashi et al. report, the other is the result of a ITRAN/ENDF/B-IV run. The third is the non elastic emission spectrum as evaluated from ENDF/B-IV data for the source group. We emphasize that these spectra are normalized each to unity, not to 1 source neutron. What we observe are, thus, purely spectral distributions.

There is no evidence of an excess of neutrons in the 6 - 8 MeV range as the experimental spectrum is compared with the calculated spectrum. The latter, we remember, is based on data assigning an evaporation distribution to both neutrons. In fact, the non elastic basic data (the third spectrum in the figure) is quite similar to the leakage spectra, all three spectra clearly showing an accumulation of neutrons about an average energy about 3 MeV.

In conclusion, we state that the Takahashi experiment shows an unusual high multiplicative power of Pb. The only consistent explanation of this high multiplicative power is to assume (i) a high σ_3/σ_2 ratio for D-T neutrons and/or (ii) a high fraction of the emission of the (n,2n) reaction falling above the (n,2n) threshold. Both these assumptions are difficult to settle with our knowledge and understanding of neutron interactions.

VI. Conclusions

The amplification of D-T neutron sources can be described in simple terms. The neutron slowing down process in the energy range from 14 MeV to the (n,2n) threshold can be approximated with a generalized slowing down equation in which the usual infinite medium slowing down collision rates are modified by average collision probabilities. With proper averaging of group-to-group cross sections and of average collision probabilities, the process can effectively be described with one, or two, group parameters.

The nuclear parameters for the approximate description of the amplification are λ^{eff} and η^{eff} , the number of neutrons generated by collisions in the amplification energy range, respectively below and in the amplification range. The geometrical parameters are P and W, the average collision probabilities for, respectively, source neutrons and first non-source generation of neutrons.

Practical formulae for W in spherical shell geometry, with the source at center, are developed. The dependence of W on the optical thickness of the shell is intimately related to the dependence of W_m on the optical thickness. W_m is the average collision probability for late neutron generations which is shown, in diffusion theory, to be intimately related to the geometrical buckling of the body in which the collision process takes place.

The effective description of the amplification as a one-group process, with its analytical expressions for the effect of multiple collisions, is helpful in deducing source-energy cross sections from measurements of total multiplications. Measurements of total multiplications and of the total leakage above the (n,2n) threshold can be combined with the analytical expressions of the theory to provide some data on the hardness of the spectrum of the secondary neutron emissions of 14 MeV source neutrons.

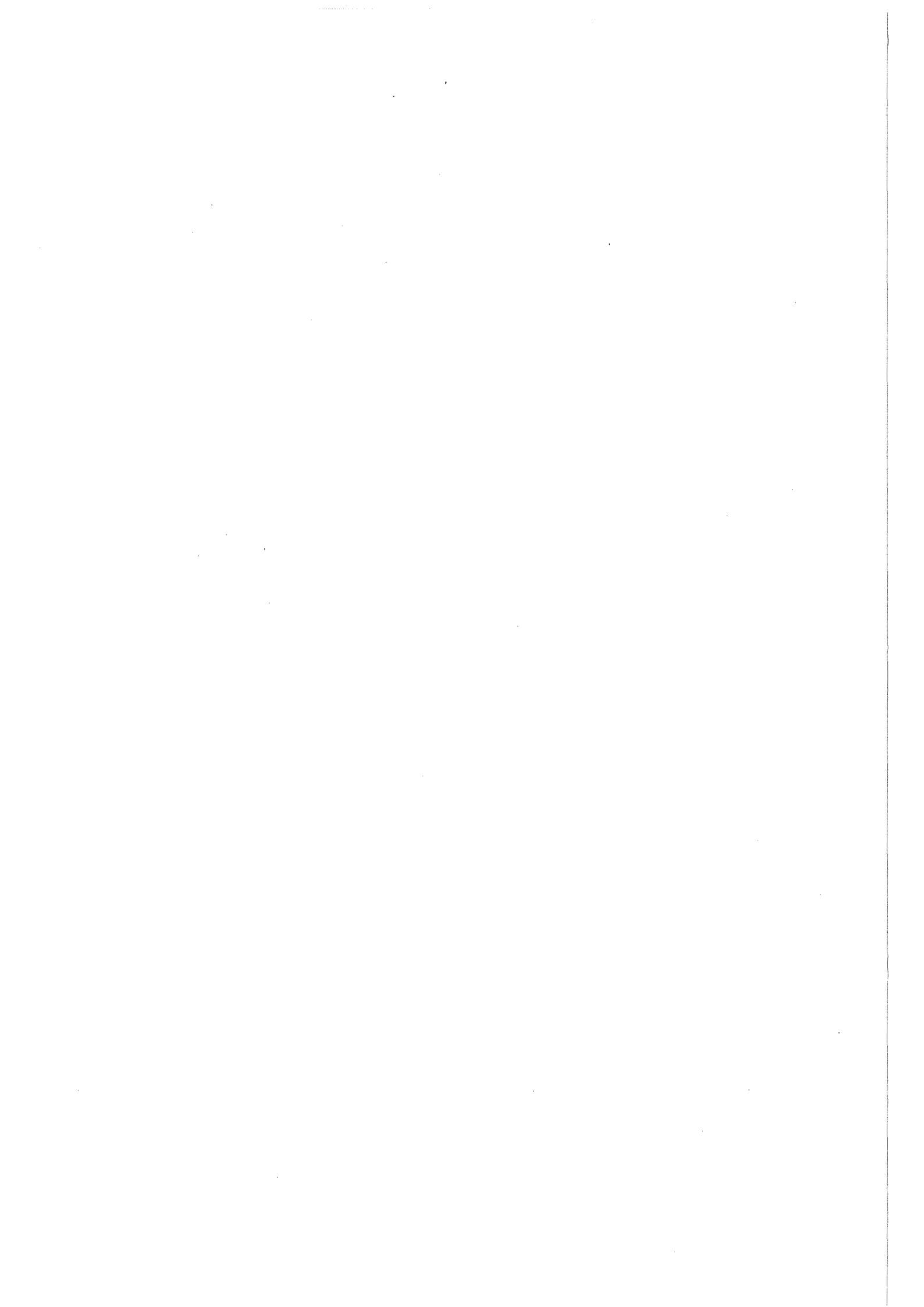
Acknowledgement

The author gratefully appreciates the opportunity of performing the presented work at the Nuclear Research Center Karlsruhe.

The efforts of Dr. H. Küsters on behalf of the research are specially acknowledged.

Mr. M. Kühle is specially thanked for comments and suggestions.

Finally I would like to thank Mrs. F. Timke for typing this manuscript.



References

- /1/ M.T.Swinhoe, C.A.Uttley,
Int. Conf. Nuclear Cross Sections for Technology, Knoxville,
Tenn. 1979, NBS. Pub.594, p.264 (1980)
- /2/ A.Takahashi et al.,
12th SOFT Symp. Fusion Technology, Jülich (1982) p.681, Pergamon Press
- /3/ V.D.Aleksandrov et al.,
Atomnaja Energija. Vol. 52, No.6, p:422, (1982)
- /4/ T.K.Basu et al.,
Nucl. Sci. Eng. 20, p.309 (1979)
- /5/ L.F.Hansen et al.,
Nucl. Sci. Eng. 72, p.35 (1979)
- /6/ J.Maniscalco,
Nucl. Techn. 28, p.98, (1976)
- /7/ H.A.Bethe, J.R.Beyster, R.E.Carter,
J. Nucl. Energy Vol. 3, p.207 (1956)
- /8/ A.M.Weinberg, E.P. Wigner,
The Physical Theory of Neutron Chain Reactors, p.705-714 (1958)
Univ. of Chicago Press
- /9/ A.Kumar,
Nucl. Sci. Eng. 81, p.66 (1982)

APPENDIX : THE AVERAGE COLLISION PROBABILITY FOR A UNIFORM, ISOTROPIC,
SMALL SPHERICAL SOURCE SHELL IN A SPHERICAL MATERIAL SHELL

The calculation of $\langle P \rangle$ is based on Fig. A.1. The smallness of source has two aspects

$$r_2 \ll R_1 \quad (\text{A.1})$$

$$\Sigma r_2 \ll 1 \quad (\text{A.2})$$

The material shell thickness, in the direction θ for a neutron generated at the point r in the source, is

$$\ell(r, \theta) = \sqrt{R_2^2 - r^2 \sin^2 \theta} - \sqrt{R_1^2 - r^2 \sin^2 \theta} \quad (\text{A.3})$$

Using (A.1) we expand the square roots in Eq.(A.3) in two terms each
The result is

$$\ell \sim \Delta + \delta(r, \theta) \quad (\text{A.4})$$

where

$$\Delta = R_2 - R_1 \quad (\text{A.5})$$

$$\delta(r, \theta) = \frac{1}{2} \left(\frac{1}{R_1} - \frac{1}{R_2} \right) r^2 \sin^2 \theta \quad (\text{A.6})$$

The collision probability for the neutron generated at r and travelling in θ is

$$P(r, \theta) = 1 - e^{-\Sigma \ell(r, \theta)} \quad (\text{A.7})$$

therefore,

$$\langle P \rangle = 1 - \langle e^{-\Sigma \ell(r, \theta)} \rangle \quad (\text{A.8})$$

where, for a uniform and isotropic source,

$$\langle \rangle \equiv \int_0^1 d(\cos \theta) \int_{r_1}^{r_2} \frac{3}{3-r_1} r^2 dr \quad (\text{A.9})$$

Using (A.4) in (A.8) we have

$$\langle P \rangle = 1 - e^{-\Sigma \Delta} \langle e^{-\Sigma \delta(r, \theta)} \rangle \quad (\text{A.10})$$

but, with (A.1) and (A.2)

$$\Sigma \delta(r, \theta) \ll 1 \quad (\text{A.11})$$

therefore

$$\langle P \rangle = 1 - e^{-\Sigma(\Delta + \langle \delta \rangle)} \quad (\text{A.12})$$

$\langle \delta \rangle$ is easily calculated from (A.6) and (A.9). The final result is

$$\langle \delta \rangle = \frac{1}{5} \frac{r_2^5 - r_1^5}{r_2^3 - r_1^3} \left[\frac{1}{R_1} - \frac{1}{R_2} \right] \quad (\text{A.13})$$

Table II.1: The Coefficient ϵ_2 in the Expression $[1 + \epsilon_1 (\text{chord}) + \epsilon_2 (\text{chord})^2]^{-1}$ for the Average Escape Probability for a Centrally Peaked Source

	Kumar's fitting		Diffusion Theory (Eq. II.14) $1 \ll \ell\Sigma$
	$0 < \ell\Sigma < 3$	$1 < \ell\Sigma < 10$	
Infinite Slab	.030	.0578	.0760
Sphere	.136	.152	.171
Cylinders $H/D \rightarrow \infty$.093	.114	.130
$H/D = 1.0$.170	.178	.204
$H/D = 0.1$.099	.089	.107
Cube	.195	.193	.228

Table II.2: Coefficients α , β , γ for the Analytical Representation of the Probabilities W_m and W for Spherical Shells

k	α	β		γ
		$0 < x < 3$	$3 < x$	
0.0	.75	.237	.304	.30
0.2	.92	.360	.454	.30
0.4	1.17	.510	.634	.27
0.6	1.47	.657	.824	.25
0.8	1.87	.847	1.020	.25
0.9	2.25	.748		.25
1.0	2.94	.580		.25

$$1 - W_m = [1 + \alpha_k x + \beta_k x^2]^{-1}$$

$$1 - W = [1 + \alpha_k x + \beta_k x^2 + \gamma_k x^3]^{-1}$$

Table II.3: The Fitted Probability W Compared with the
Accurate Probability

Upper figures - W (accurate) in parts per thousand
 lower figures - [W (fitted) - W (accurate)] in
 parts per thousand

x \ k	0.0	0.2	0.4	0.6	0.8	0.9	1.0
.1	68* +4	91* -2	110* -1	130* +3	153* +8	186* -10	230* -38
.2	140* +1	175* -6	210 -6	244 0	289 -3	325 -16	390* -57
.4	270* -3	322* -11	368 -7	415 0	473 -4	509 -12	560* -34
.8	488* -8	535* -6	585 -3	633 0	681 0	707 -2	735* -5
1.2	636* +3	680* -1	721 -1	757 +2	793 +1		828* +2
1.6	742* +8	777* +2	809 -1	837 -2	861 -1		883* +2

*values taken from a graph in Bethe's article; non starred
 figures are values read from tabulations in Bethe's article.

Table II.4: Values of the Parameter β_K as Determined from the Application of the Diffusion Relation (Eq. II.9) to Transport-Theory Bucklings

k	0.	0.2	0.4	0.6	0.8	1.0
Fitted $0 < x \leq 1.6$ Diffusion Appr.	.237	.360	.510	.657	.847	.580
→ 0.	.304	.396	.513	.652	.844	1.216
= 1.	.304	.413	.556	.730	.945	1.216
→ ∞	.304	.454	.634	.824	1.020	1.216

Table III.I.a: Pb Data

Group	<Energy> MeV	σ_{tr}	η_{el}	η	λ	ξ
Source	14.2	3.059	.186	.280	1.434	.174
2	12.9	3.113	.199	.279	1.409	.012
3	11.6	3.211	.216	.282	1.356	.016
4	10.5	3.217	.216	.260	1.317	.013
5	9.5	3.273	.222	.258	1.172	.019
6	8.6	3.326	.229	.252	.962	.016
7	7.8	3.326	.234	.256	.811	.015
8	7.1	3.386	.230	.230	.783	.015

Table III.1.b: Zr Data

Group	<Energy> MeV	σ_{tr}	η_{el}	η	λ	ξ
Source	14.2	1.93	.088	.184	1.412	.086
2	12.9	1.98	.100	.174	1.364	.023
3	11.6	2.02	.106	.185	1.108	.008
4	10.5	2.07	.114	.178	1.103	.010
5	9.5	2.12	.120	.189	.985	.010
6	8.6	2.16	.138	.196	.857	.009
7	7.8	2.23	.150	.211	.796	.015
8	7.1	2.36	.190	.190	.803	.023

Table III.1.c: Cu DATA

Group	<Energy>	σ_{tr}	η_{el}	η	λ	ξ
Source	14.2	1.85	.088	.149	1.055	.089
2	12.9	1.86	.128	.150	.987	.055
3	11.6	1.92	.092	.150	.814	.004
4	10.5	1.94	.097	.098	.826	.001

Table III.1.d: Fe DATA

Group	<Energy> MeV	σ_{tr}	η_{el}	η	λ	ξ
Source	14.2	1.67	.092	.183	.950	.092
2	12.9	1.64	.150	.171	.892	.082
3	11.6	1.71	.091	.092	.904	.009

Table III.1.e: U238 Data

Group	<Energy> MeV	σ_{tr}	η_{el}	η	λ	ξ
Source	14.2	3.23	.126	.182	2.634	.126
2	12.9	3.26	.139	.185	2.515	.011
3	11.6	3.40	.143	.190	2.163	.014
4	10.5	3.48	.154	.187	2.056	.013
5	9.5	3.55	.155	.183	1.993	.012
6	8.6	3.60	.156	.178	1.929	.006
7	7.8	3.67	.161	.180	1.783	0.
8	7.1	3.76	.173	.193	1.489	0.
9	6.4	3.84	.184	.184	1.153	0.

Table III.1.f: Be Data

Group	<Energy> MeV	σ_{tr}	η_{el}	η	λ	ξ
Source	14.2	.950	.315	.989	.532	.048
2	12.9	.818	.206	1.066	.485	.267
3	11.6	1.03	.328	1.110	.412	.095
4	10.5	1.08	.334	1.028	.474	.121
5	9.5	1.16	.356	.984	.488	.076
6	8.6	1.20	.357	.978	.479	.048
7	7.8	1.22	.356	.976	.470	.038
8	7.1	1.25	.354	.971	.528	.034
9	6.4	1.30	.344	.918	.494	.038
10	5.8	1.34	.400	.838	.551	.037
11	5.0	1.28	.378	.638	.741	.072
12	4.1	1.42	.388	.573	.732	.059
13	3.3	1.77	.490	.490	.694	.029
14	2.7	1.95	.160	.160	.857	.027

Table III.2: Effective One- and Two-Group Parameters for Multipliers
of D-T Neutron Sources

Material	Group	Energy Extension (MeV)	σ_{tr} (barns)	Number of Secondaries Emitted		
				$\rightarrow 1$	$\rightarrow 2$	$\rightarrow (\langle B_2^* \rangle)$
U238	1	14.9 - 6.1	3.23	.191		2.637
Pb	1	14.9 - 6.7	3.06	.260		1.430
ZR	1	14.9 - 6.7	1.93	.128		1.472
CU	1	14.9 - 10.0	1.85	.135		1.070
FE	1	14.9 - 11.1	1.67	.156		.975
BE	1	14.9 - 13.5	0.95	.048	.941	.560
	2	13.5 - 2.5	1.21		.850	.376

* B_2 here means the bottom energy of group 2 in Be,
or bottom energy of group 1 in the other materials

Table III.3.a : Amplification in Pb

Δ (cm)	k	x	P	W	ITRAN RESULTS			(1 GROUP/ITRAN)-1 %		
					M-1	L	H	M-1	L	H
.2	.980	.0202	.0203	.0526	.0144	.0290	.986	-1.6	+1.2	-0.1
.5	.952	.0505	.0498	.115	.0359	.0724	.963	-1.3	+1.4	-0.1
1.0	.909	.101	.0971	.193	.0714	.144	.927	-1.2	+1.4	-0.3
3.0	.769	.303	.264	.386	.205	.417	.788	+0.5	-1.4	-0.6
9.0	.526	.909	.599	.656	.502	1.03	.470	-0.7	+0.1	-0.9
15.0	.400	1.51	.782	.795	.685	1.42	.268	-0.7	-0.5	+0.9
25.0	.286	2.53	.922	.907	.833	1.73	.105	-0.2	-0.1	+2.4
50.0	.167	5.05	.994	.981	.917	1.91	.0087	+0.4	0.0	

Table III.3.b: Amplification in Zr

$\Delta(\text{cm})$	k	x	P	W	ITRAN RESULTS					
					(1 GROUP/ITRAN)-1			%		
					M-1	L	H	M-1	L	H
0.2	.980	.0164	.0165	0.432	.00909	.0235	.986	+0.4	+4.0	-0.1
1.0	.909	.0822	.0797	.162	.0488	.116	.932	+0.1	+3.0	-0.4
3.0	.769	.247	.220	.332	.140	.341	.800	-1.4	-0.5	+0.1
9.0	.526	.739	.525	.588	.343	.836	.508	-0.8	0.0	-0.6
15.0	.400	1.23	.711	.731	.469	1.15	.320	+0.4	+0.2	-1.1
50.0	1.67	4.11	.984	.968	.667	1.65	.0193	+0.3	+1.2	+3.2

Table III.3.c : Amplification in Cu

$\Delta(\text{cm})$	k	x	P	W	ITRAN RESULTS			(1 GROUP/ITRAN)-1 %		
					M-1	L	H	M-1	L	H
.2	.980	.0314	.0313	.0797	.00647	.0334	.973	0.0	+1.1	0.0
1.0	.909	.154	.1467	.214	.0312	.162	.869	+0.3	+0.8	-0.1
3.0	.769	.470	.378	.514	.0835	.436	.648	-0.2	-0.3	+0.2
9.0	.526	1.41	.759	.791	.173	.910	.263	+0.7	-0.1	+0.8
15.0	.400	2.35	.906	.901	.209	1.104	.1050	+1.1	0.0	+2.6
50.0	.167	7.84	.9996	.996	.231	1.231	.00037	+2.3	+0.4	

Table III.3.d: Amplification in Fe

Δ (cm)	k	x	P	W	ITRAN RESULTS			(1 GROUP/ITRAN)-1 %		
					M-1	L	H	M-1	L	H
.2	.980	.0284	.0284	.0727	.00382	.0275	.976	-1.3	+2.0	0.0
.5	.952	.0711	.0695	.155	.00949	.0681	.941	-1.7	+1.8	-0.1
1.0	.909	.142	.134	.254	.0186	.134	.884	-1.7	+1.0	-0.2
3.0	.769	.427	.350	.484	.0504	.368	.683	-1.5	+0.4	-0.3
9.0	.526	1.28	.725	.763	.108	.801	.307	-0.1	+0.1	-0.3
15.0	.400	2.13	.883	.882	.133	.997	.136	+0.7	+0.1	+0.2
25.0	.286	3.56	.972	.960	.148	1.114	.0338	+1.3	0.0	+4.2
50.0	.167	7.11	.9992	.994	.152	1.151	.0009	+1.7	+0.1	

Table III.3.e: Amplification in U238

$\Delta(\text{cm})$	k	x	P	W	ϵ	ITRAN RESULTS			(1 GROUP/ITRAN)-1 %		
						M-1	ϵL	H	M-1	ϵL	H
.2	.980	.0291	.0290	.0742	1.0069	.0542	.0770	.977	+0.3	+1.5	-0.1
.5	.952	.0727	.0710	.1578	1.0155	.136	.193	.943	+0.3	+1.5	-0.2
1.0	.909	.145	.137	.258	1.0268	.274	.387	.887	-0.4	+0.5	-0.4
3.0	.769	.436	.356	.400	1.0592	.791	1.103	.688	-1.5	-0.5	-0.8
9.0	.526	1.31	.732	.770	1.116	1.85	2.54	.311	-0.9	-0.5	-1.7
15.0	.400	2.18	.888	.886	1.148	2.38	3.24	.138	-0.2	0.0	-2.0
25.0	.286	3.63	.974	.9617	1.173	2.71	3.67	.0341	+0.5	+0.4	+2.1
50.0	.167	7.27	.9993	.995	1.186	2.82	3.82	.00120	+1.4	+1.0	

Table III.3.f : Amplification in Be

group	Δ (cm)	k	x	P	W	ITRAN RESULTS			(1 GROUP/ITRAN)-1 %		
						M-1	L	H	M-1	L	H
1	.2	.980	.0228	.0228	.0591	.0131	.0135	.9996	-1.2	-0.4	0.0
2			.0326		.0741						
1	1.0	.909	.114	.1090	.213	.0669	.0730	.9938	+2.1	+2.1	0.0
2			.163		.258						
1	3.0	.769	.342	.292	.419	.223	.264	.9584	-2.7	-3.3	+0.3
2			.490		.490						
1	9.0	.526	1.026	.644	.695	.694	.933	.762	-2.0	-3.9	+2.9
2			1.47		.769						
1	15.0	.400	1.711	.821	.829	1.075	1.53	.546	+4.4	+2.3	+3.4
2			2.45		.886						
1	50.0	.167	5.70	.997	.989	1.81	2.76	.0501	+9.5	+6.0	+7.2
2			8.16		.992						

Table IV.1 : Iterated Number of Secondaries Emitted in the Multiplication Region; Eq. (IV.7)

Shell Thickness (cm)	Be $\eta^{(1)}$: iterated from $\nu^{(0)}=1.56$	Be $\eta^{(1)}$: iterated from $\nu^{(0)}=1.52$	Pb $\eta^{(1)}$: iterated from $\nu^{(0)}=1.70$
1	.55	.72	.150
3	.69	.76	.209
9	.71	.74	.226
15	.70	.73	.233
50	.70	.72	.230

Table V.1: Multiplications, Partial Multiplications, and Derived Quantities from the Takahashi's Experiment on Pb Spherical Shells

Shell outer thickness (cm)	Multiplication per one source neutron							
	0 - 0.3 MeV	0.3 - 4 MeV	4 - 7 MeV	H 7 - 15 MeV	M 0 - 15 MeV	M-1	$\zeta = \frac{M-H}{M-1}$	$\left 1 - \frac{\zeta}{\langle \zeta \rangle} \right $
3	.074	.420	.025	.775	1.294 \pm .01	.294	1.77	4.7 %
6	.183	.760	.036	.584	1.563 \pm .01	.563	1.74	3.0 %
9	.250	1.050	.040	.500	1.840 \pm .03	.840	1.59	5.9 %
12	.336	1.190	.038	.372	1.936 \pm .09	.936	1.67	1.2 %
							$\langle \zeta \rangle = 1.69$	

Fig. II.1: $\frac{W_m}{(1-W_m)x}$ and $\frac{W}{(1-W)x}$ for a Sphere

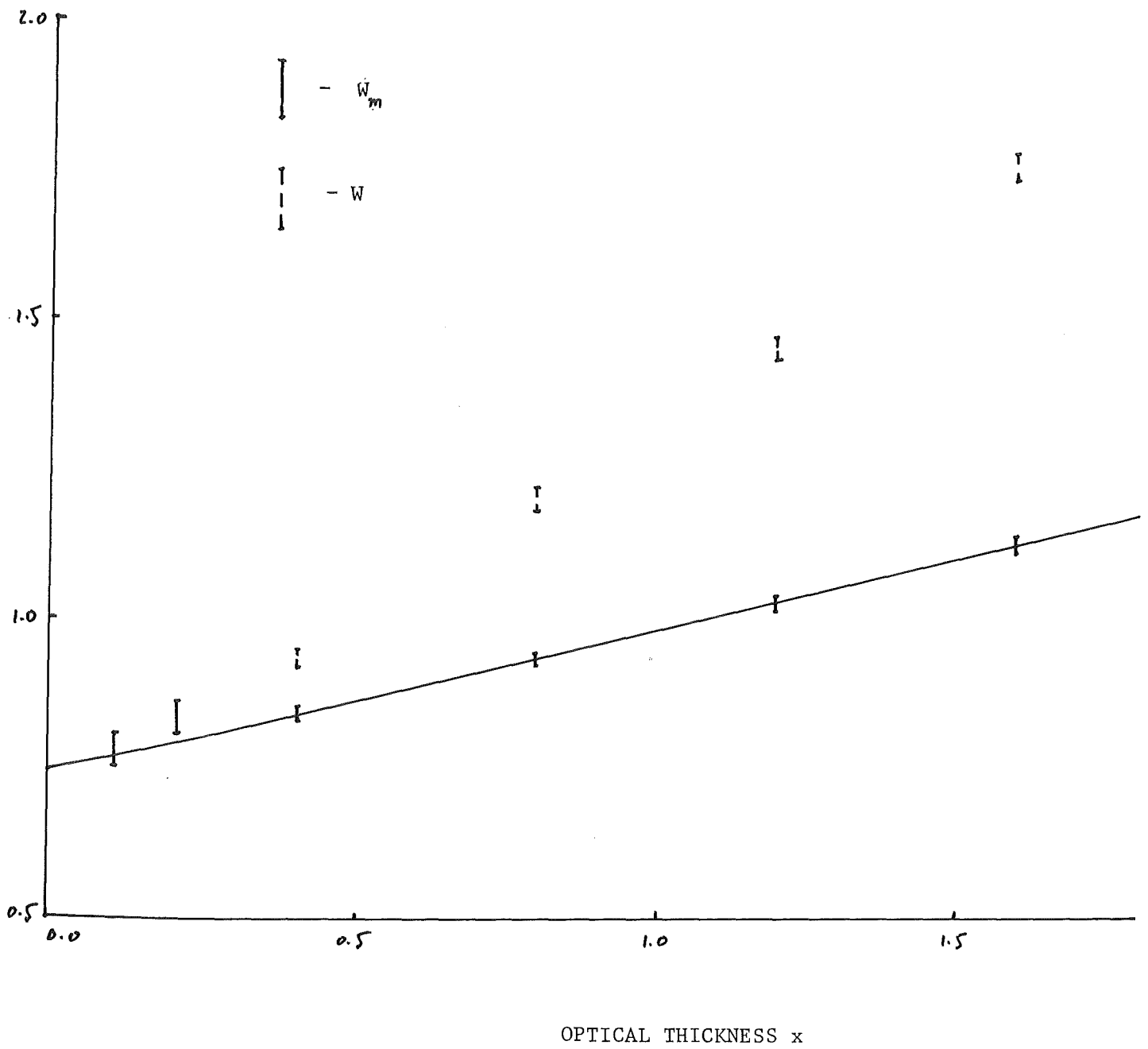


Fig. II.2: $\frac{W_m}{(1-W_m)x}$ and $\frac{W}{(1-W)x}$ for a Spherical

Shell with $R1/R2 = 0.2$

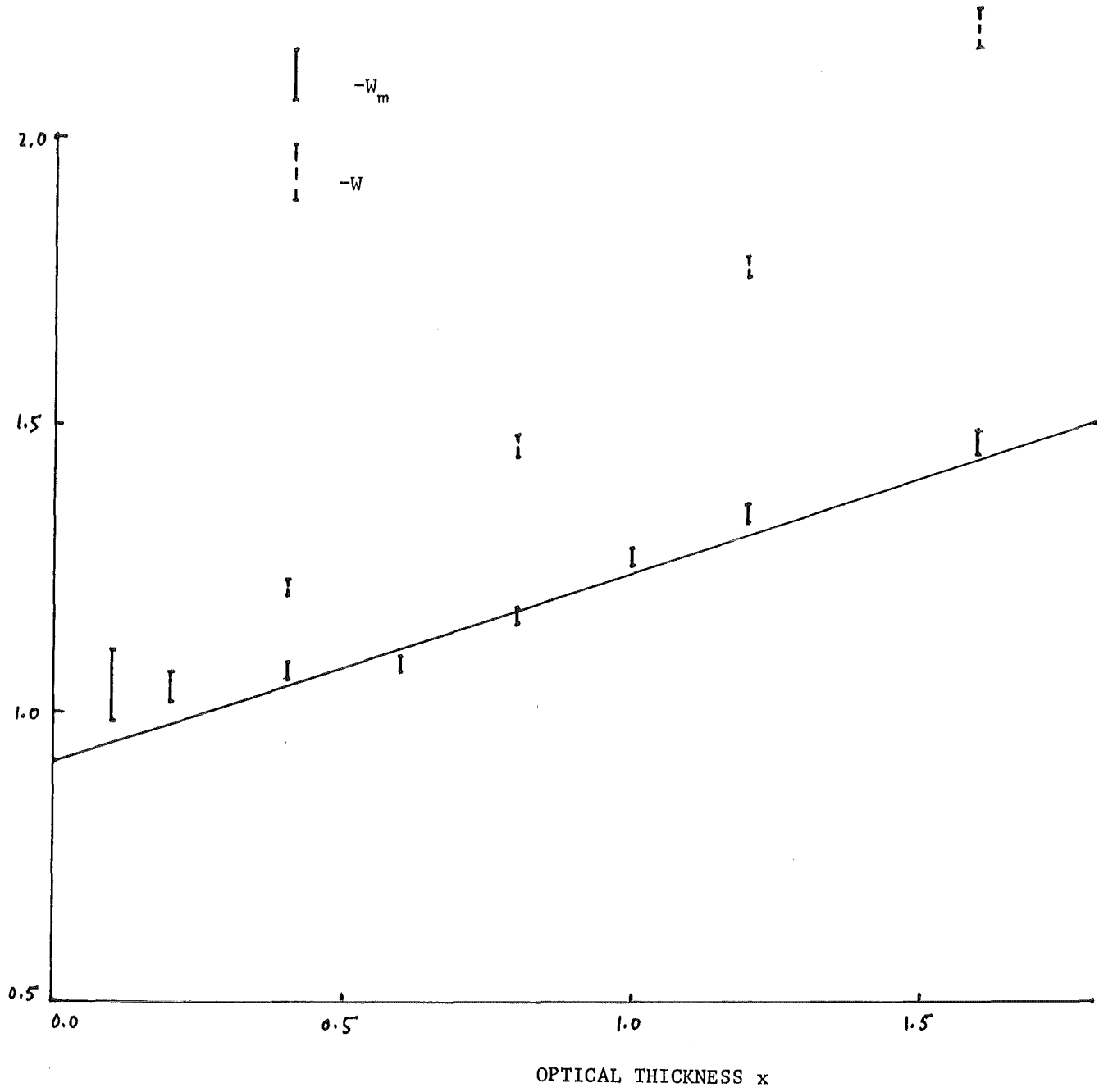


Fig. II.3: $\frac{W_m}{(1-W_m)x}$ and $\frac{W}{(1-W)x}$ for a Spherical

Shell with $R_1/R_2 = 0.4$

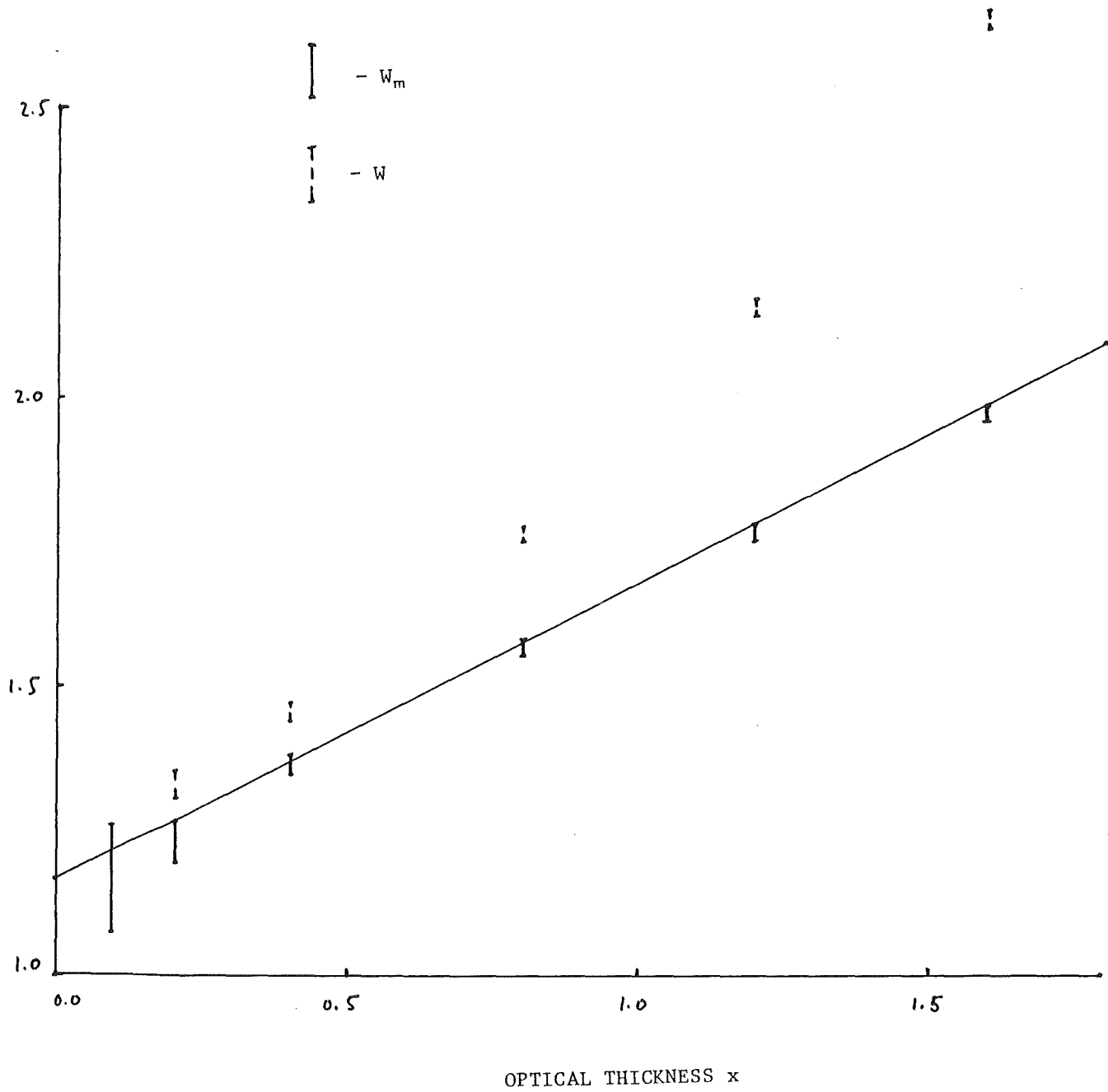


Fig. II.4: $\frac{W_m}{(1-W_m)x}$ and $\frac{W}{(1-W)x}$ for a Spherical

Shell with $R_1/R_2 = 0.6$

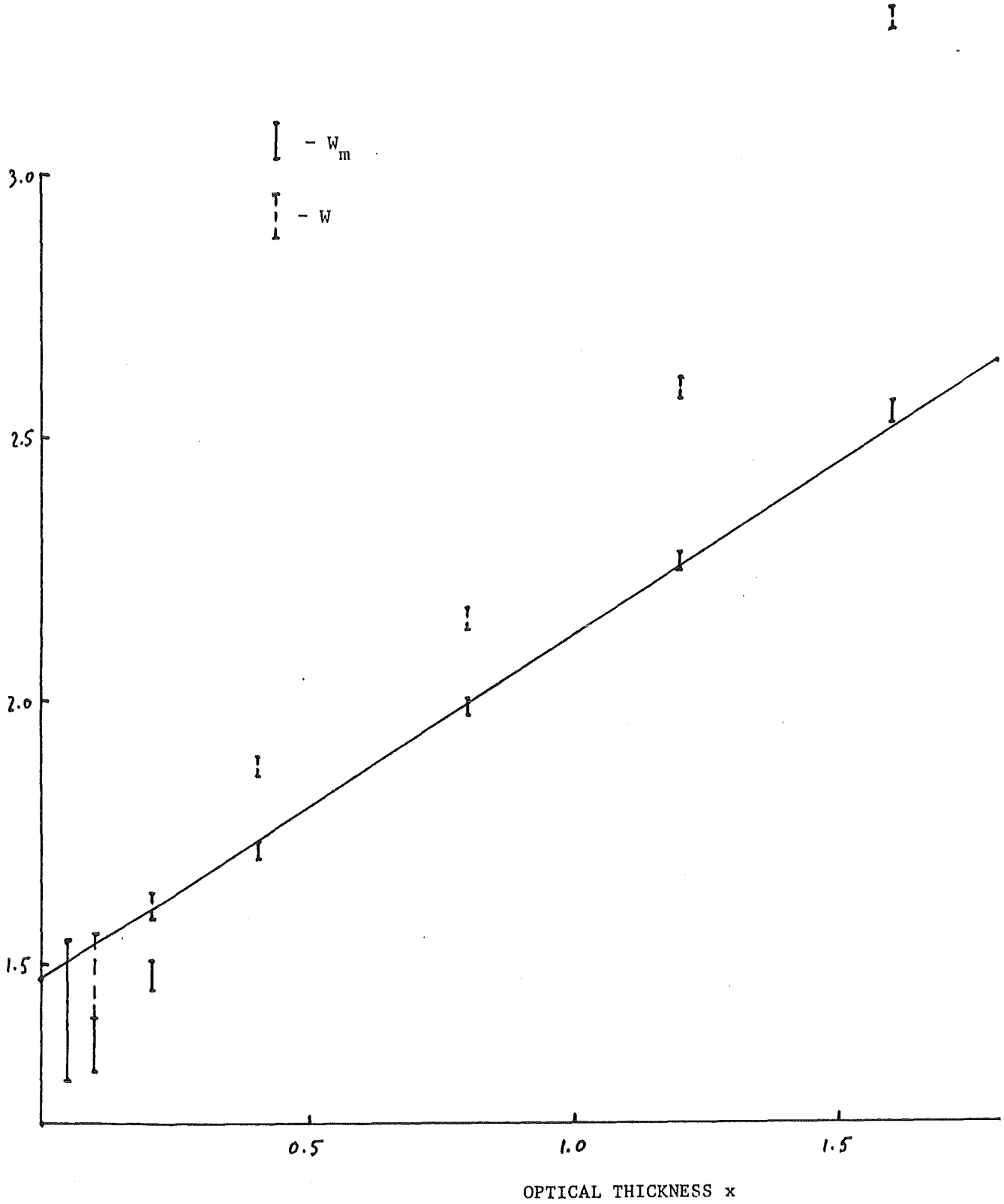


Fig. II.5: $\frac{W_m}{(1-W_m)x}$ and $\frac{W}{(1-W)x}$ for a Spherical

Shell with $R1/R2 = 0.8$

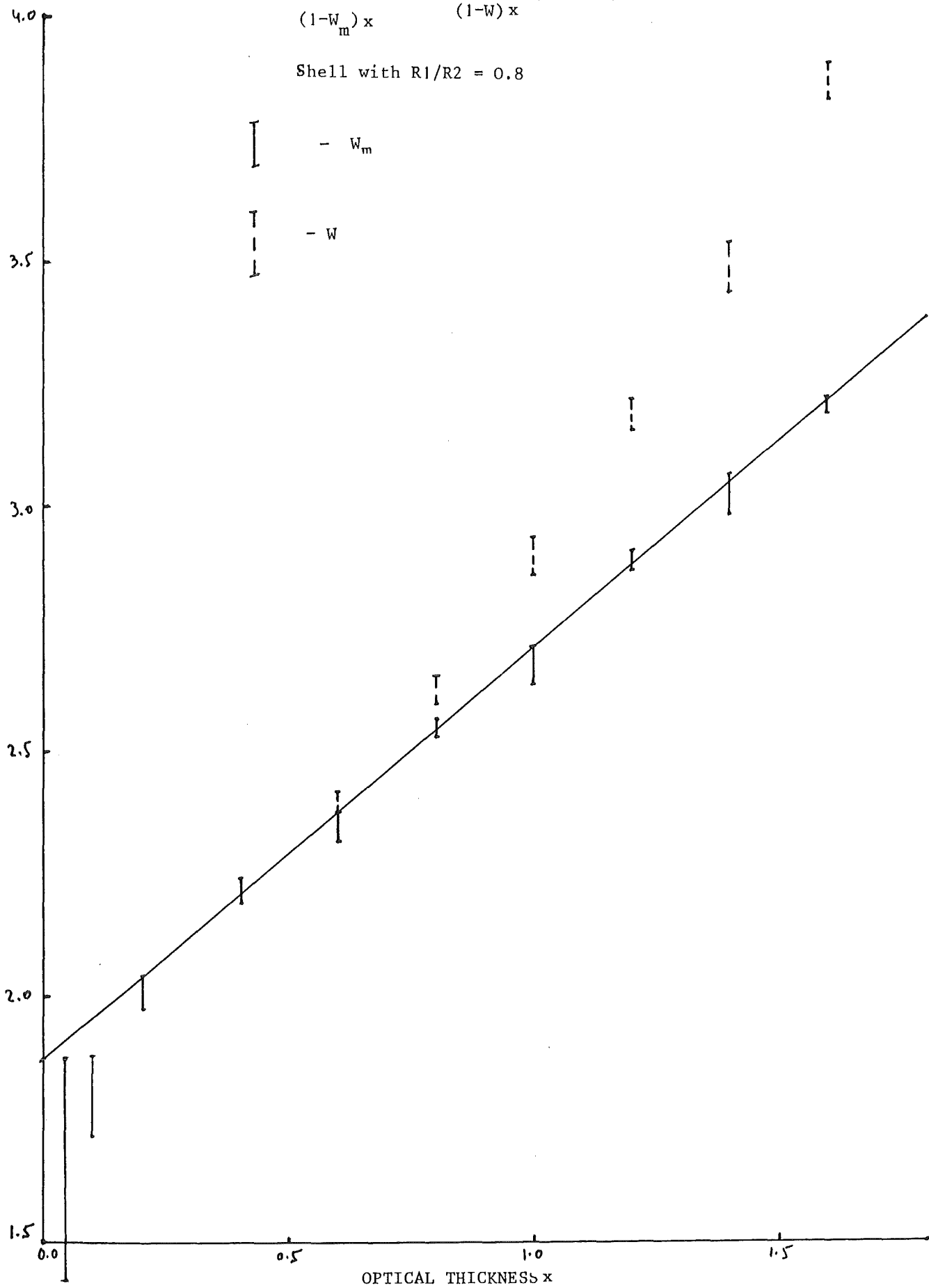
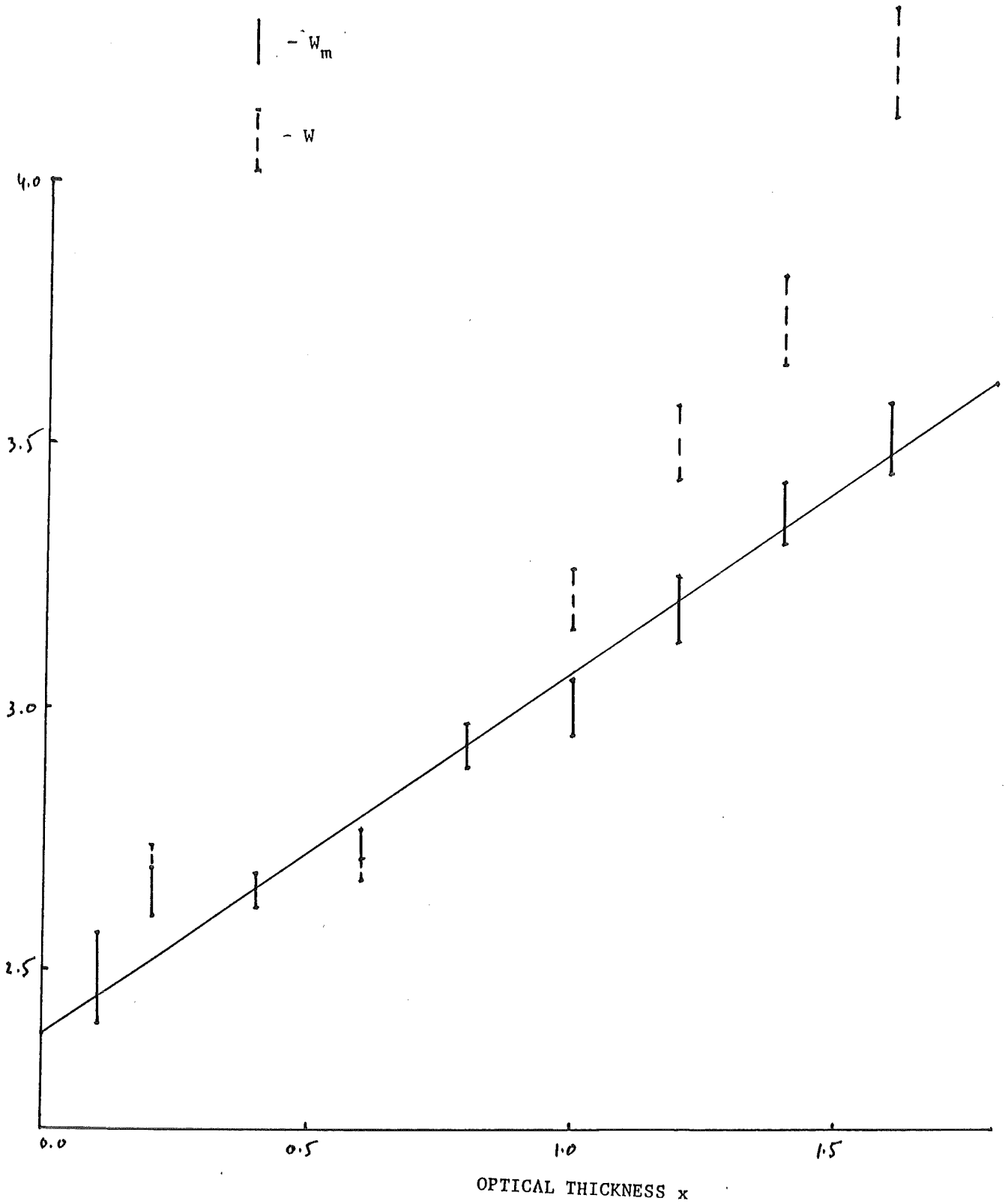


Fig. II.6: $\frac{W_m}{(1-W_m)x}$ and $\frac{W}{(1-W)x}$ for a Spherical

Shell in the limit $R_1/R_2 \rightarrow 1$



COLLISION
(% per MeV)

Fig. III.1: Energy Distribution of the Space-Integrated Collision Rate of Non-Source Neutrons in Be

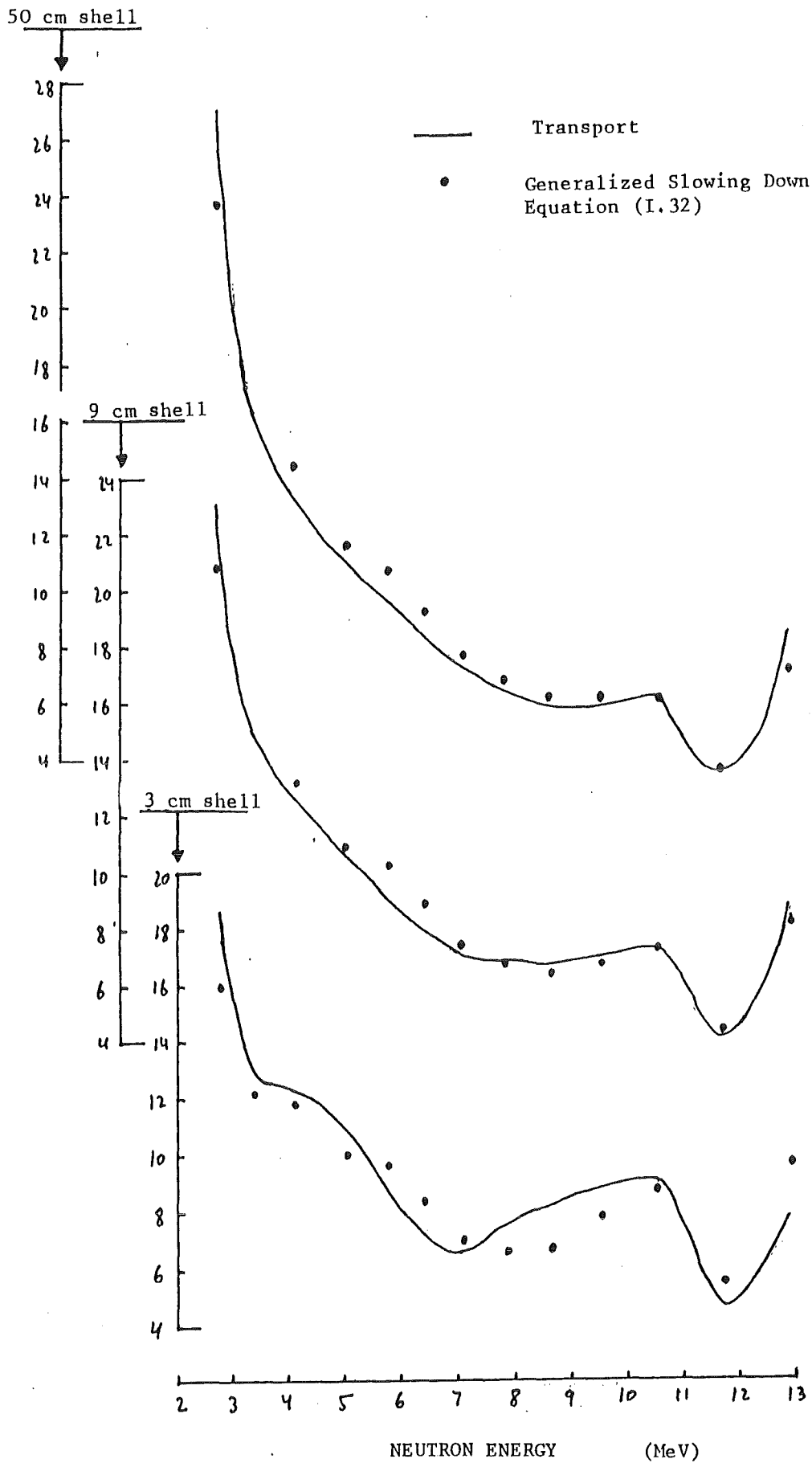


Fig. IV.1: Extrapolation to Zero to determine the Number of Secondaries in U238

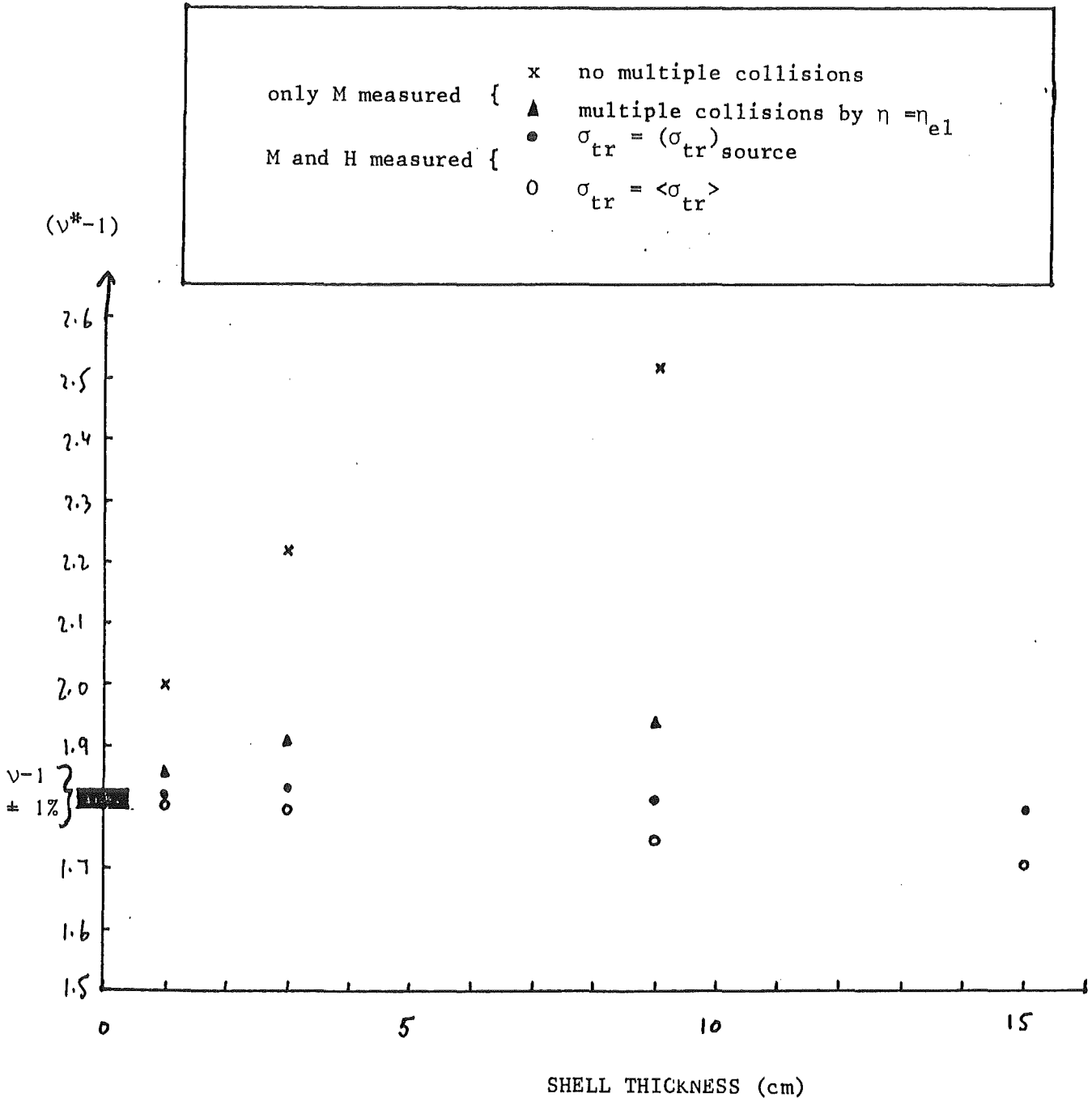


Fig. IV.2: Extrapolation to Zero to determine the Number of Secondaries in Pb

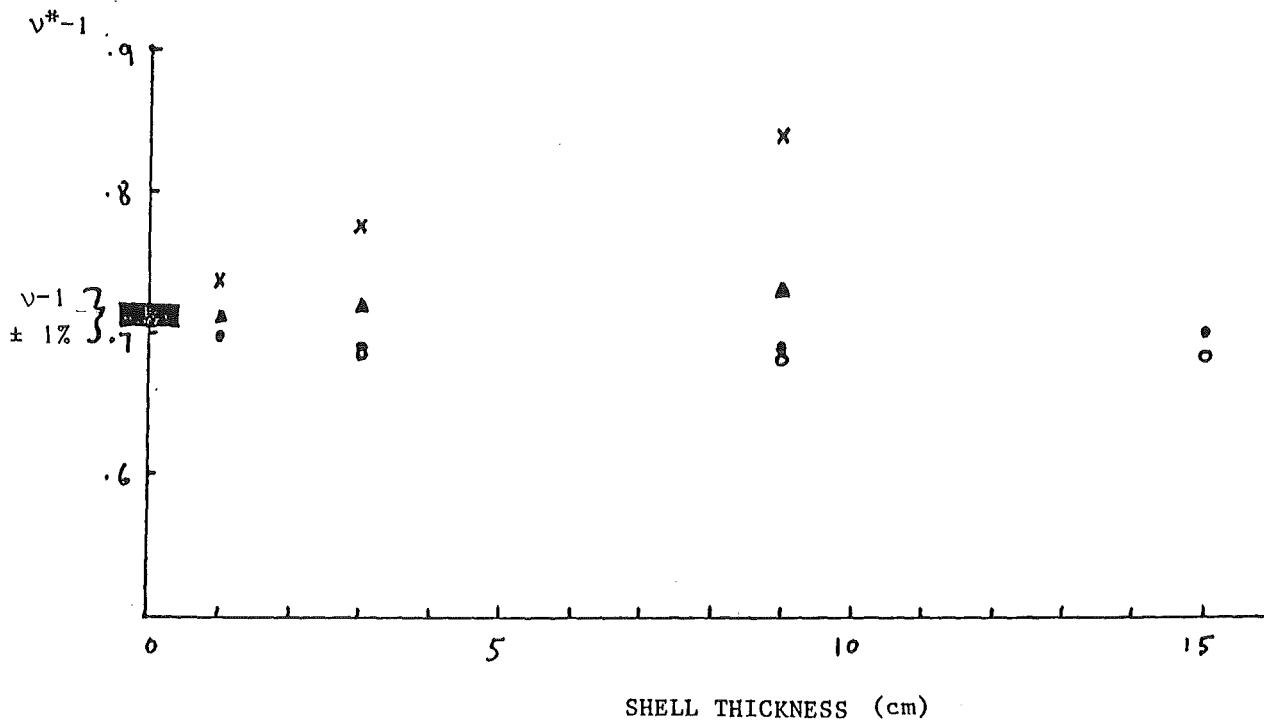
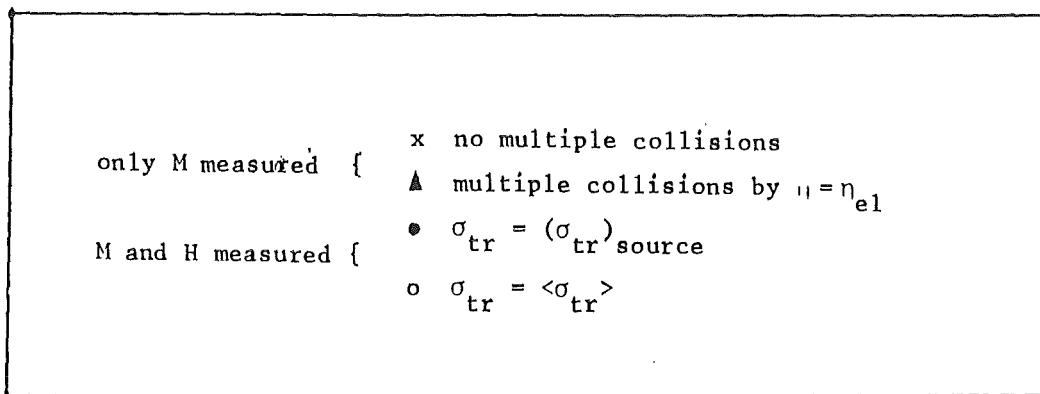


Fig. IV.3: Extrapolation to Zero to determine the Number of Secondaries in Be

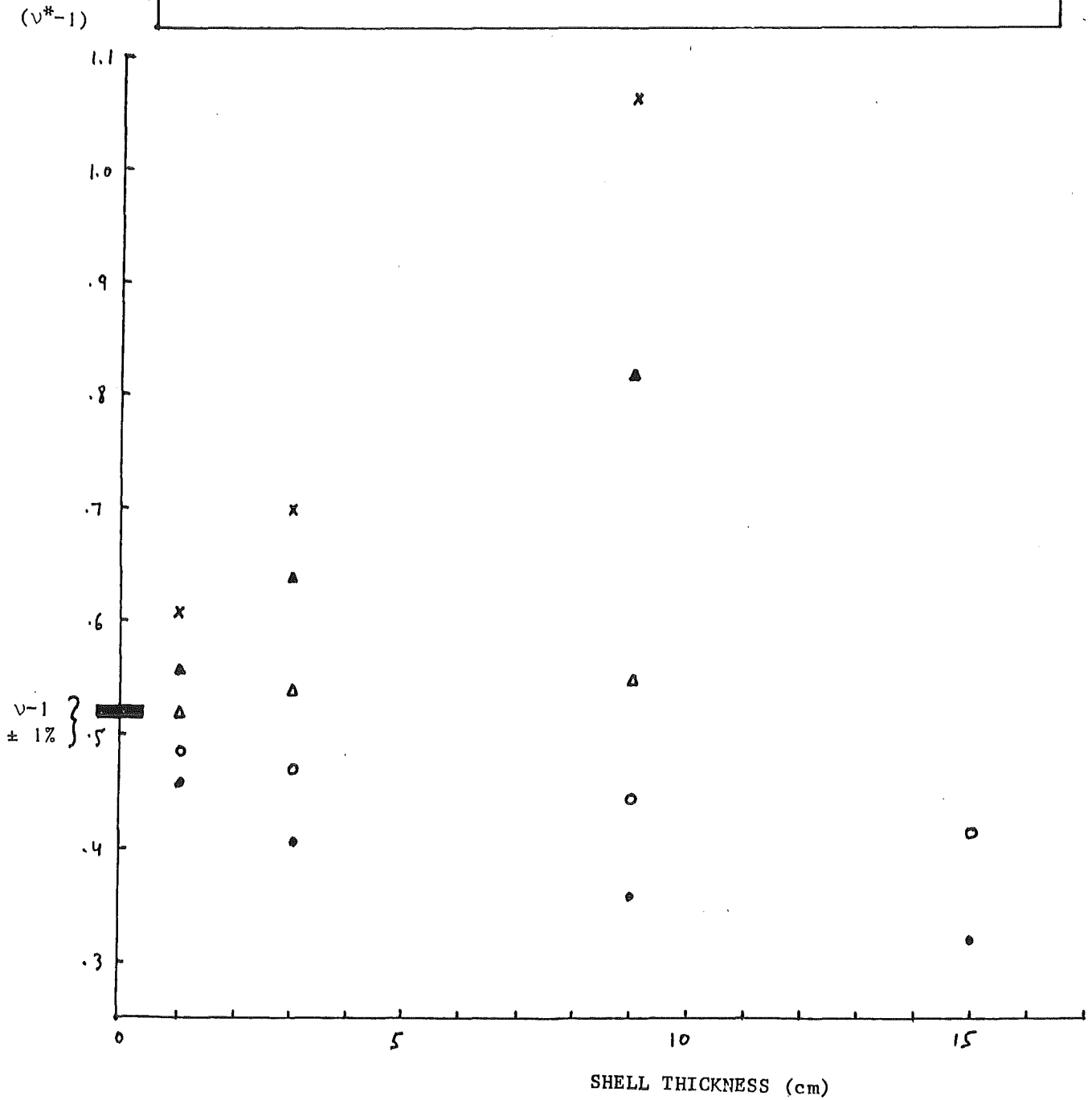
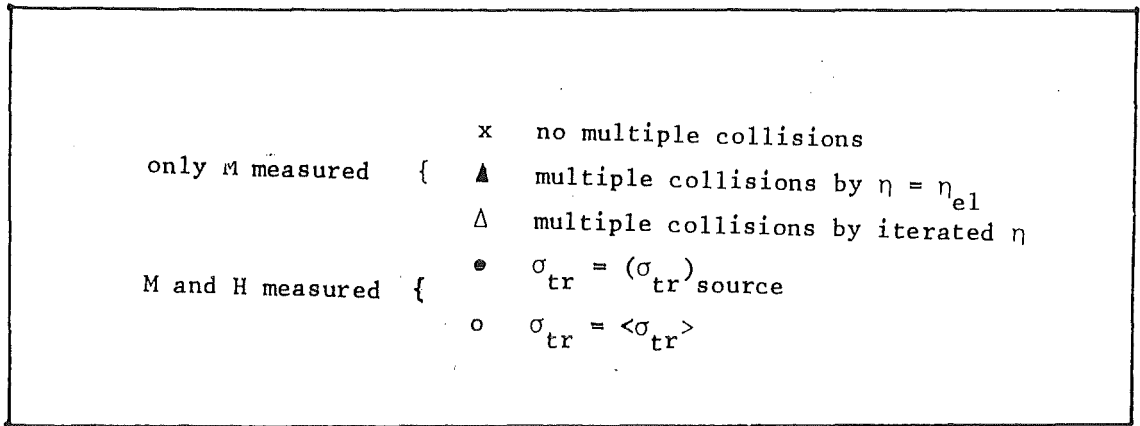


Fig. IV.4: Effective Number of Secondaries Emitted in Be above the (n,2n) threshold

M and H measured { \bullet $\sigma_{tr} = (\sigma_{tr})_{source}$
 \circ $\sigma_{tr} = \langle \sigma_{tr} \rangle$

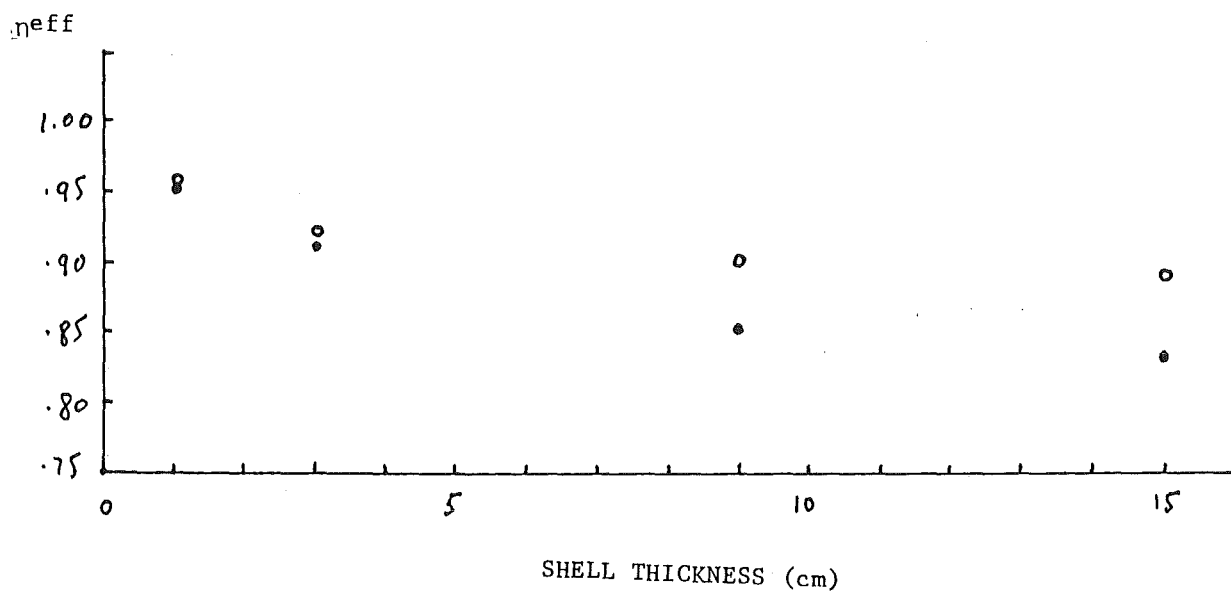


Fig. V.1: Attempts to fit Experimental Multiplications with

$f_2^* = 0, \sigma = 4$

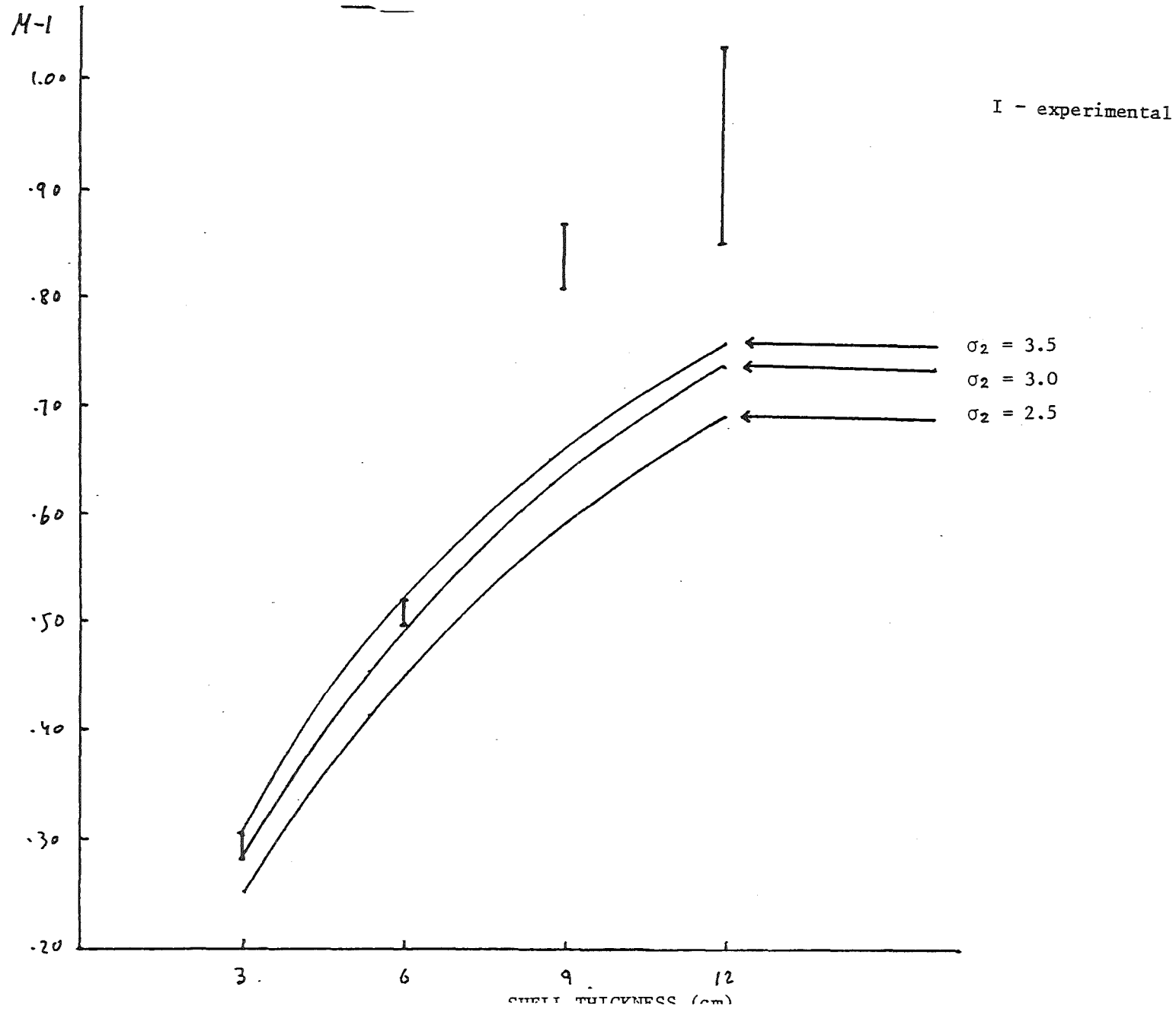


Fig. V.2: Attempts to fit Experimental Multiplications with

$$f_2^* = 0, \sigma = 5$$

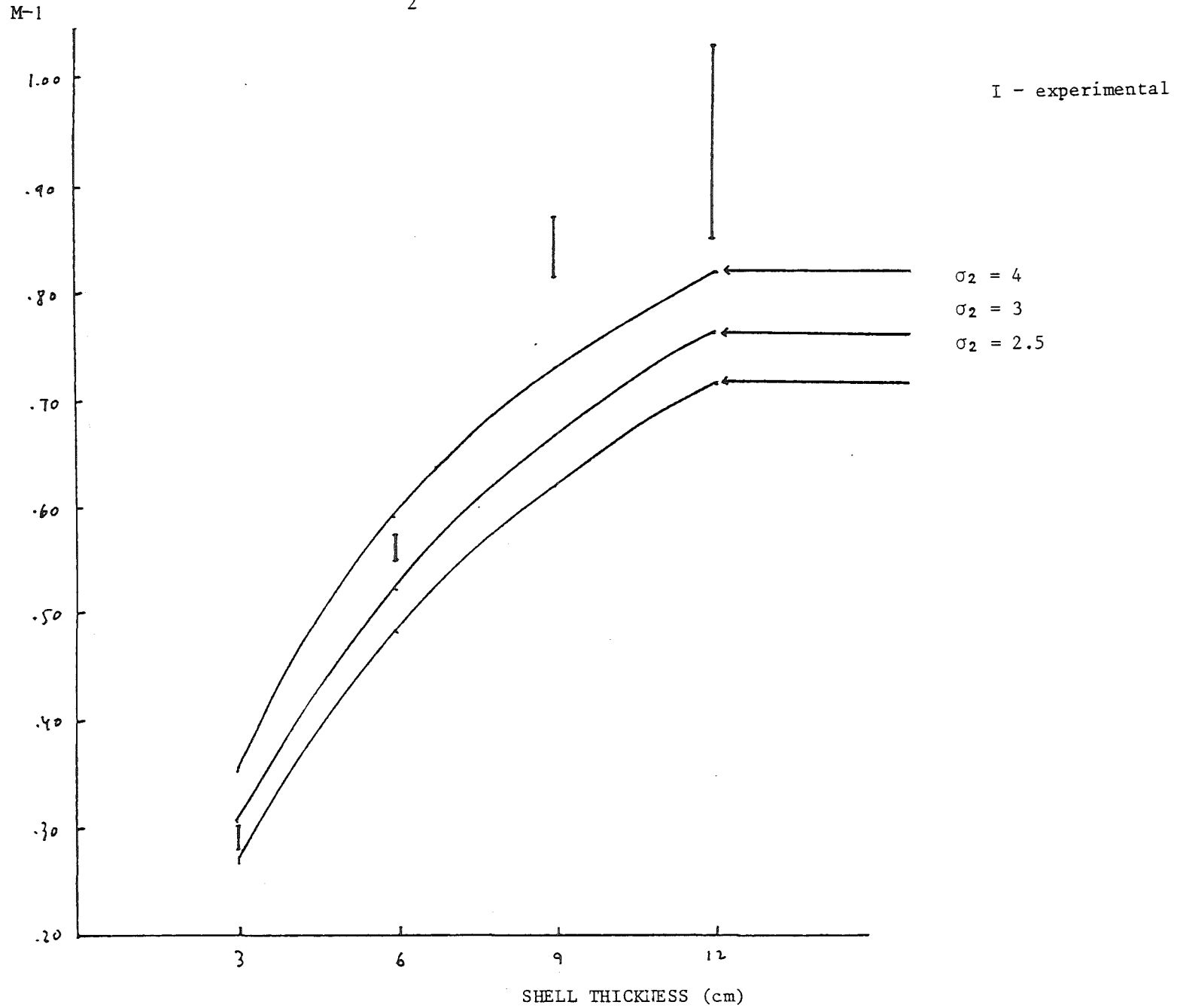


Fig. V.3: Attempts to fit Experimental Multiplications
with $f_2^* = 0.10$

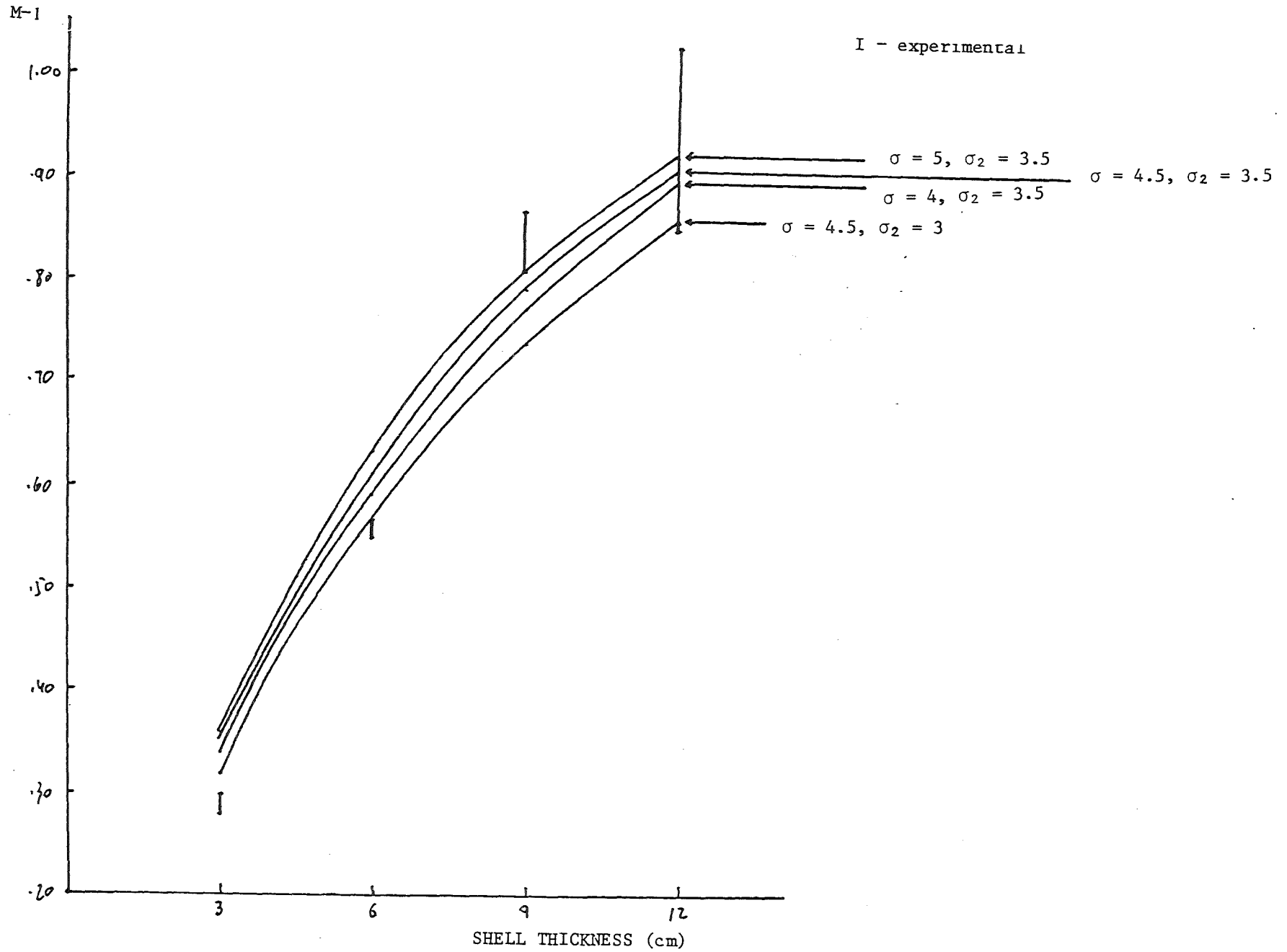


Fig. V.4: Attempts to fit Experimental Multiplications with $f_2^* = 0.20$

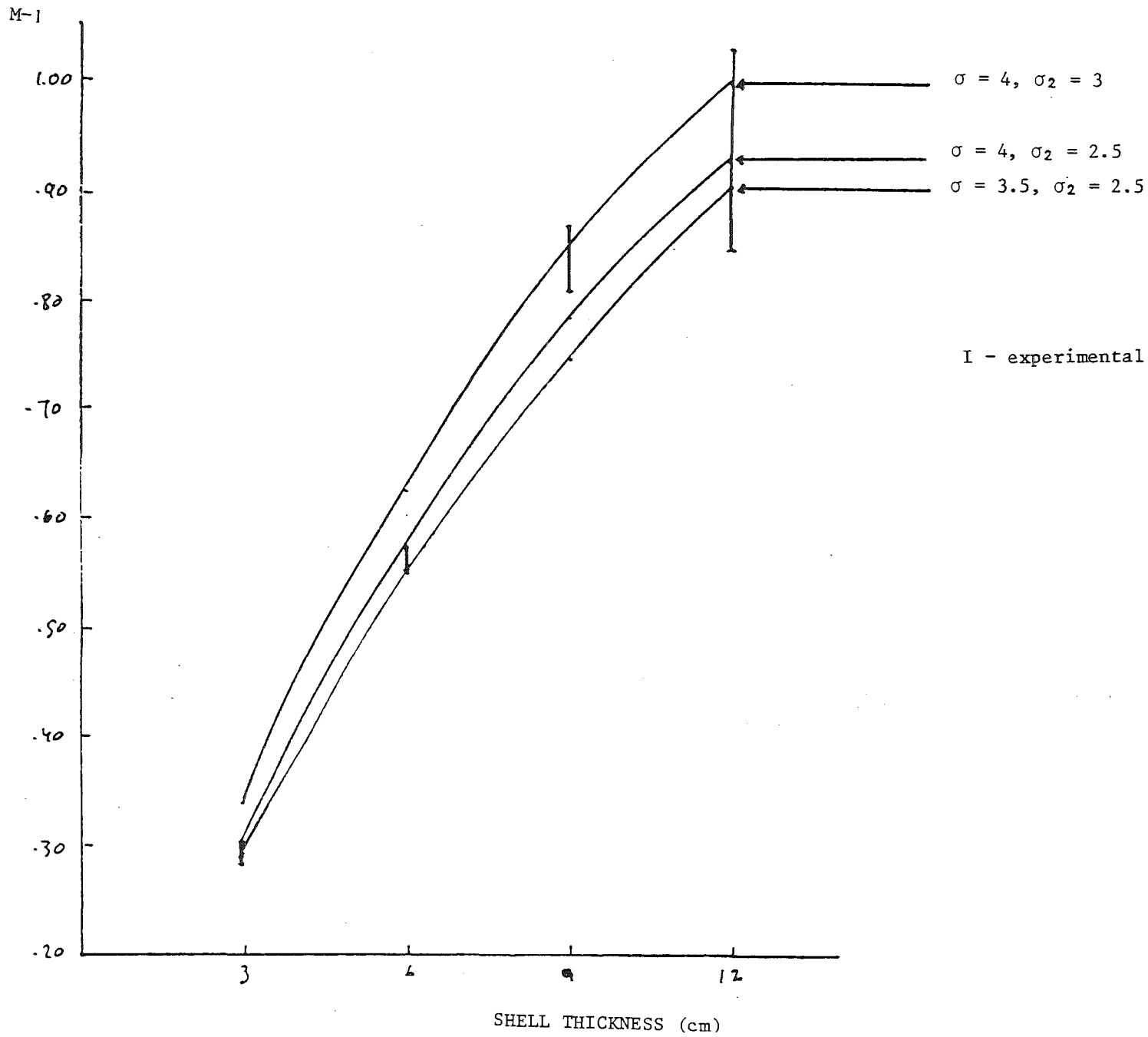
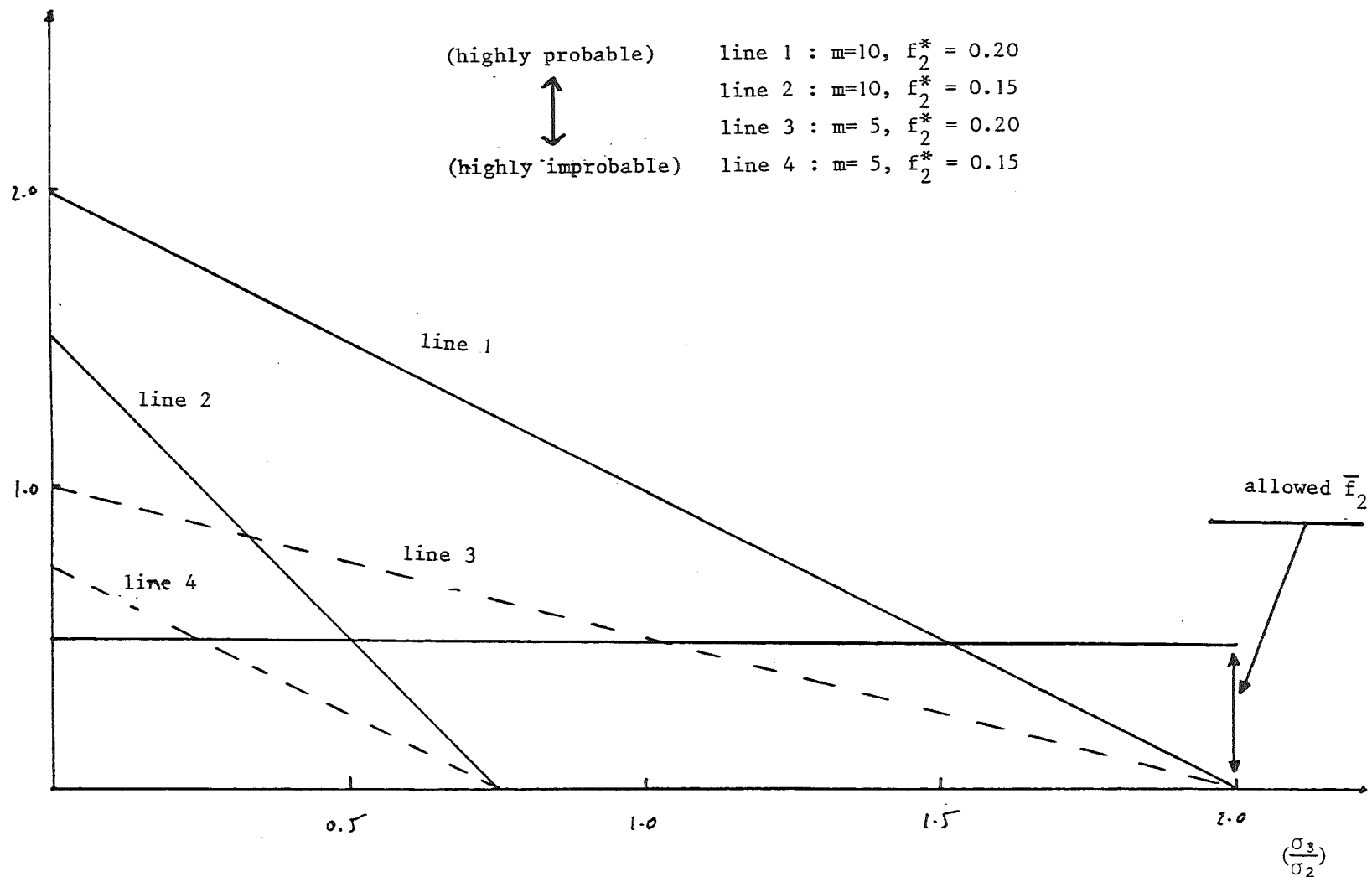


Fig. V.5: Interdependence of \bar{f}_2 and $\frac{\sigma_3}{\sigma_2}$ for the Analysis of the Takahashi Experiment

\bar{f}_2 - fractions of (n,2n) secondaries emitted above the (n,2n) threshold



spectrum
fraction

Fig. V.6: Neutron Spectrum per unit lethargy

(each spectrum integral from 0.3 to 12 MeV is 1)

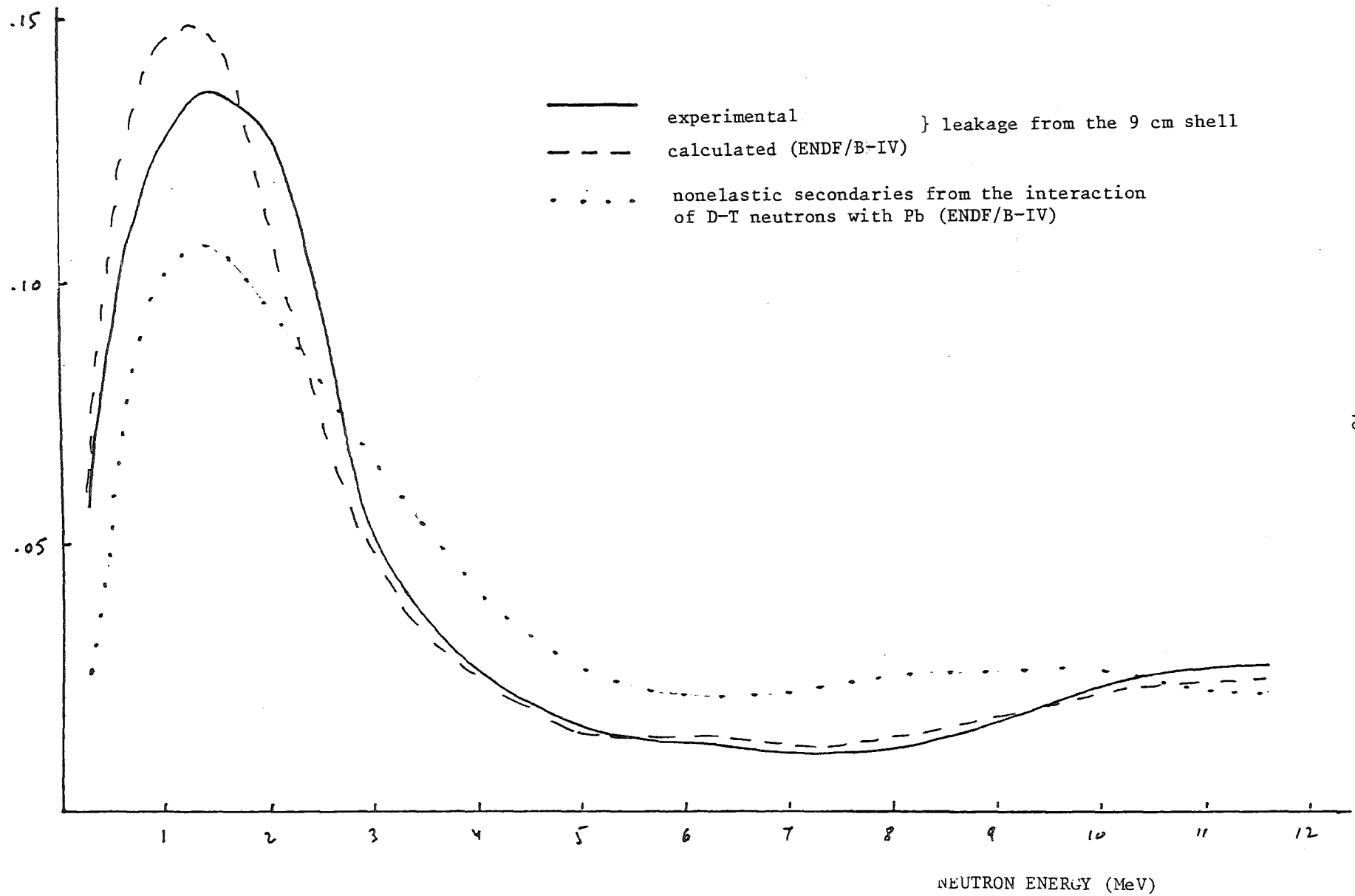


Fig. A.1: A Spherical Neutron Source-Shell
Material-Shell

